TÜRKİYE CUMHURİYETİ
ADANA ALPARSLAN TÜRKEŞ SCIENCE AND TECHNOLOGY UNIVERSITY

GRADUATE SCHOOL OF NATURAL AND APPLIED SCIENCES
DEPARTMENT OF BIOENGINEERING

DEVELOPMENT OF EPITOPE IMPRINTED ANTIMICROBIAL CRYOGEL DISCS FOR TANNIC ACID RELEASE

BÜŞRA TUNA

M.Sc.

ADANA 2024

TÜRKİYE CUMHURİYETİ
ADANA ALPARSLAN TÜRKEŞ SCIENCE AND TECHNOLOGY UNIVERSITY

GRADUATE SCHOOL OF NATURAL AND APPLIED SCIENCES
DEPARTMENT OF BIOENGINEERING

DEVELOPMENT OF EPITOPE IMPRINTED ANTIMICROBIAL CRYOGEL DISCS FOR TANNIC ACID RELEASE

BÜŞRA TUNA

M.Sc.

THESIS ADVISOR
PROF. DR. GÖZDE BAYDEMİR PEŞİNT

ADANA, 2024

CERTIFICATION OF APPROVAL

DEVELOPMENT OF EPITOPE IMPRINTED ANTIMICROBIAL CRYOGEL DISCS FOR TANNIC ACID RELEASE

This **M.Sc.** thesis, **completed under the conditions determined by the relevant regulations**, by **Büşra TUNA with student number** 19500301009 in **Adana Alparslan Türkeş Science and Technology University Institute of Graduate School** Bioengineering **Department**, has been evaluated by the following academic committee, and approved in accordance with the relevant articles of the "Adana Alparslan Türkeş Science and Technology University Graduate Education Regulations".

Prof. Ahmet BEYCİOĞLU
Institute of Graduate School Manager

Prof. Gözde BAYDEMİR PEŞİNT
Head of the Department

Prof. Gözde BAYDEMİR PEŞİNT
Academic Advisor

Assoc. Prof. Hatice İmge OKTAY BAŞEĞMEZ
Academic Co-supervisor

Thesis Advisory Committee Members
Prof. Dr. Gözde BAYDEMİR PEŞİNT
Adana Alparslan Türkeş Science and Technology University

Prof. Ayşe Müge ANDAÇ
Hacettepe University

Assoc. Prof. Dilek GÖKTÜRK
Adana Alparslan Türkeş Science and Technology University

Assoc. Prof. Benay TUNÇSOY
Adana Alparslan Türkeş Science and Technology University

Assoc. Prof. Hatice İmge OKTAY BAŞEĞMEZ
Adana Alparslan Türkeş Science and Technology University

Thesis Defence Date

22/01/2

ÖZET

TANNİK ASİT SALIMI İÇİN EPİTOP BASKILANMIŞ ANTİMİKROBİYAL KRİYOJEL DİSKLERİN GELİŞTİRİLMESİ

Büşra TUNA
Yüksek Lisans, Biyomühendislik Anabilim Dalı
Danışman: Prof. Dr. Gözde BAYDEMİR PEŞİNT
II. Danışman: Doç. Dr. Hatice İmge OKTAY BAŞEĞMEZ
Ocak 2024, 54 sayfa

Moleküler baskılama yöntemi, istenen moleküle duyarlı polimerlerin sentezlenmesine olanak tanır. Kriyojeller, bu polimerlerden biri olup çözücünün donma sıcaklığı altında üretilen jel matrisleridir. Kriyojeller, por yapıcı malzeme olarak toksik organik bileşikler içermeyip, bunun yerine por yapıcı malzeme olarak buz kristallerini kullanır. Doğal malzemelerle desteklenen kriyojeller, biyouyumluluk, esneklik ve yüksek mekanik kararlılık gibi avantajlar sunar, bu da onları yara iyileşmesi, doku iskeleti oluşturma, ilaç salımı gibi birçok uygulamada destekleyici bir tedavi yöntemi haline getirir. Bu araştırmada, Tannik asit molekülünün antimikrobiyal etkilerinden faydalanarak epitop baskılanmış kriyojel disklerin hazırlanması amaçlanmaktadır. Bu diskler, akut yara iyileştirici ve antimikrobiyal özelliklere sahip bir biyomalzemenin literatüre kazandırılmasını hedefler. Jelatin yapılı gallik asit baskılanmış biyouyumlu kriyojeller üretilmiş ve bu kriyojellerin yapısına farklı konsantrasyonlarda tannik asit eklenerek antimikrobiyal özellik kazandırılması amaçlanmıştır. Sentezlenen kriyojeller FTIR, şişme testleri ve SEM ile karakterize edilmiştir. Ayrıca, farklı konsantrasyonlardaki tannik asit yüklenmiş kriyojel disklerden tannik asidin kümülatif salımı ve disklerin *S. aureus* ve *E. coli* üzerindeki antimikrobiyal özellikleri değerlendirilmiştir. Yapılan çalışmalar, polimerdeki ilaç yükleme oranının arttıkça salım hızının da arttığını göstermektedir. Güç yasasına göre, salım mekanizmasının türünü gösteren "n" üsteli 0.5'ten küçük bulunmuş, bu da hazırlanan kriyojel disklerde difüzyon mekanizmasının non-Fickian olduğu sonucuna varmamıza yardımcı olmuştur.

Anahtar Kelimeler: Epitop baskılı polimerler, kriyojel diskler, tannik asit, kontrollü ilaç salım sistemleri, yara iyileşmesi

ABSTRACT

DEVELOPMENT OF EPITOPE IMPRINTED ANTIMICROBIAL CRYOGEL DISCS FOR TANNIC ACID RELEASE

Büşra TUNA
M.Sc., Department of Bioengineering

Supervisor: Prof. Dr. Gözde BAYDEMİR PEŞİNT
Co-supervisor: Assoc. Dr. Hatice İmge OKTAY BAŞEĞMEZ
January 2024, 54 pages

The molecular imprinting method allows for the synthesis of polymers sensitive to the desired molecule. Cryogels, one of these polymers, are gel matrices produced below the freezing temperature of the solvent. In contrast to many polymers containing toxic organic compounds as pore-forming agents, cryogels utilize ice crystals as the pore-forming material. Cryogels supported structurally by natural materials offer advantages such as biocompatibility, flexibility, and high mechanical stability, making them suitable for various applications like wound healing, tissue scaffolding, and drug release. In this study, the aim is to take advantage of the antimicrobial effects of Tannic acid molecules by preparing epitope-imprinted cryogel discs. These discs are intended to introduce a biomaterial with acute wound healing and antimicrobial properties to the literature. Biocompatible cryogels imprinted with gallic acid were prepared, and the goal was to impart antimicrobial properties by incorporating Tannic acid at different concentrations into the structure of the cryogels. The synthesized cryogels were characterized using FTIR, swelling tests, and SEM. Additionally, the cumulative release of Tannic acid from cryogel discs at different concentrations and their antimicrobial properties against *S. aureus* and *E. coli* were evaluated. The studies revealed that as the drug loading rate in the polymer increased, the release rate also increased. According to the power law, the exponent "n" was found to be less than 0.5, suggesting that the release mechanism in the prepared cryogel discs is non-Fickian diffusion.

Keywords: Epitope-imprinted polymers, cryogel discs, tannic acid, controlled drug release systems, wound healing

Dedication

This thesis dedicated to my beloved husband and family, who always loving and supporting me.

ACKNOWLEDGEMENTS

I would like to express my sincere thanks to my esteemed supervisor Prof. Gözde BAYDEMİR PEŞİNT, who have always guided me and provided their endless support with them experience and understanding throughout my graduate education and thesis work.

I would like to thank co-supervisor Assoc. Dr. Hatice İmge OKTAY BAŞEĞMEZ to support me during my thesis and share her knowledge.

I would like to thank my deary teammate/friend Pırıl ARISOY to support me at all stages of my thesis, thanks for her kindness and patience.

I would like to thank my dear teammates Okan ZENGER, Burcu EREN YÜNGEVİŞ, Kardelen CEMEK, Ece KAYA and Ayşe Naz CERİT who have never spared their help and support during my thesis work.

I would also like to thank my dear husband Oğuzhan TUNA, mother and father Nurcan KIZILCIK and Rıdvan KIZILCIK , my lovely sister Buket KIZILCIK, my grandmothers Halime KIZILCIK and Habibe GÜNEŞ, my grandfathers Veli KIZILCIK and İsmail GÜNEŞ, mother in law Fadime TUNA and father in law Zekeriya TUNA for their valuable support and understanding throughout my thesis studies and who have always stood by me under all circumstances.

TABLE OF CONTENTS

LIST OF FIGURES

LIST OF TABLES

LIST OF ABBREVIATIONS

TA	: Tannic Acid
GA	: Gallic Acid
MIP	: Molecularly Imprinted Polymer
MIT	: Molecular Imprinting Technology
QS	: Quorum Sensing
AHL	: Acylated Homoserine Lactone
HPLC	: High-performance liquid chromatography
ABDV	: Azobis Dimethyl Valeronitrile
AIBN	: 2,2'-azobis(isobutyronitrile)
PAHs	: Polycyclic Aromatic Hydrocarbons
PVA	: Poly(Vinyl Alcohol)
VIM	: 1- vinylimidazole
HEMA	: 2- hydroxyethyl methacrylate
p(HEMA)	: Poly(2-Hydroxyethylmethacrylate)
EGDMA	: Ethylene Glycol Dimethacrylate
APS	: Ammonium Persulfate
TEMED	: N,N,N’,N’-tetramethylene diamine
DI	: Deionized water
PBS	: Phosphate - buffered saline
NaCl	: Sodium Chloride
FTIR	: Fourier transform infrared spectroscopy
SEM	: Scanning Electron Microscope
NIP	: Non-imprinted Nanoparticle
UV	: Ultraviolet
MHA	: Mueller-Hinton Agar

LIST OF SYMBOLS

µL **:** Microliter

µm **:** Micrometer

nm **:** Nanometer

mL **:** Milliliter

mg **:** Milligram

ng **:** Nanogram

pg **:** Picogram

cm **:** Centimeter

L **:** Liter

T **:** Temperature

sec **:** Second

min **:** Minute

h **:** Hour

eq. **:** Equation

M **:** Molarity

°C **:** Celsius degree

CO_2 **:** Carbon Dioxide

1. INTRODUCTION

One such chemical that encapsulates the qualities of being safe and environmentally beneficial as well as being an effective reducing and stabilizing agent is tannic acid (TA), a polyphenolic compound obtained from woody and herbaceous plants (Božič et al., 2012). Apart from leather and dye, which are the main areas of use, tannins are used to clarify wine and beer, to increase the fluidity of drilling mud in oil wells and to prevent the formation of deposits on the walls of steam boilers (Chaplin et al., 1985). It is a naturally occurring phenolic acid group tannin that has ten molecules of gallic acid connected to a central glucose unit (Aelenei et al., 2009). TA has several uses, particularly in the areas of food and health. Due to its unique physicochemical characteristics, numerous recent investigations have demonstrated that TA is an efficient medication additive that can be used in contemporary drug delivery systems (Andrade et al., 2006).

Since TA is a natural substance found in various plants and has various properties such as antimutagenic, antioxidant, anticancer, antibacterial, it has been accepted since ancient times and used in many fields of both ancient and modern science and technology (Chaplin et al., 1985; Ahmad, 2014; Kim et al., 2010). Because of its hydroxyl groups, TA can also interact with macromolecules and biopolymers. This characteristic makes it an attractive pharmacological candidate (Sagbas et al., 2015). TA can also neutralize free radicals, which are responsible for the onset of a number of diseases, including allergies, diabetes, Parkinson's, Alzheimer's, and cardiology. TA, which displays bioactive qualities and improves the properties of materials for biomedical purposes, is now being explored as an organic polymer addition. As an antioxidant, TA is well known for its capacity to scavenge free radicals and other dangerous chemicals from living things, defending cells from oxidative damage. (Ahmad, 2014; Nakamura et al., 2003). A range of harmful bacteria and viruses, including Escherichia coli, Klebsiella pneumonia, Listeria monocytogenes, Staphylococcus aureus, Helicobacter pylori, HIV, and influenza, are inhibited by TA's antimicrobial action. Reduced microbial enzyme activity, rupture of the microbial cell membrane, and deprivation of metal ions, substrate, and minerals have all been linked to the inhibitory action of TA on microorganisms (Dai et al., 2014; Dabbaghi et al., 2019).

Several industries that are related to human health, such as hospitals and dental equipment, food packaging and storage, water filtration systems, and domestic hygiene, are highly concerned about contamination by microorganisms. A wide range of illnesses and diseases have been caused by the dangerous microorganisms that exist in these places. Antibiotic resistance's quick development makes things more difficult (Lode, 2009; Mcdonnel & Russell, 1999). For this reason, efforts are being made to develop new macromolecules with antimicrobial properties by structural modification of the known polymer in order to obtain a desired biological and physicochemical property in order to decontaminate the areas and to get rid of microorganisms (Jain et al., 2014). Antimicrobial polymers are substances with the power to eradicate or stop the development of bacteria on a surface or in the immediate environment (Kenawy et al., 2007). Low molecular weight antimicrobial agents have many disadvantages such as toxicity to the environment and short-term antimicrobial ability, antimicrobial polymer studies eliminate these disadvantages and offer an effective solution (Glekman, 2001; Palza, 2015).

Smart drug delivery systems have captured the interest of researchers in the biomedical and pharmacological areas over the past ten years. Scientists have started to use release systems in therapeutic agents like proteins as well as in the pharmaceutical sector as a result of the development of new materials and technologies. Increasing drug safety and therapeutic efficacy is the goal of all controlled release systems (Park, 2014; Langer, 1993). In controlled drug release, it is aimed to release the drug at the optimum value in a stable manner over a long period of time, without distinction of high or low dose (Huang et al., 2004). At this point, molecular imprinting technology is widely used. The three-dimensional interactions between the template molecule, the functional monomer, and the crosslinker around it are the foundation of the technology known as molecular imprinting (Mosbach & Ramström, 1996). Using these kinds of interactions, a technique known as molecular imprinting allows synthetic polymers to recognize predefined ligands and imitate the recognition events seen in biomolecular recognition processes (Wackerlig & Schirhagl, 2016). The affordability and suitability of molecularly imprinted polymers (MIP) for molecular recognition is a huge benefit. High temperature, pressure, and a broad pH range are all physical and chemical conditions to which MIPs are extremely robust. MIPs can also be kept for a long time and utilized frequently (Owens et al., 1999).

Cryogels, whose material potential was discovered in the early 1970s; They are three-dimensional gel matrices prepared with partially frozen monomeric or polymeric solutions. They are macroporous or super macroporous gels with spongy morphology (Okay, 2014). It is ideal to believe that the cryogelation process happens in stages. Ice crystal formation, cross-linking and phase separation by polymerization, and the development of interconnecting pores following the dissolution of ice crystals are the four topics that can be addressed (Rogers & Bencherif, 2019). When forming cryogels, first of all, a molecule (ligand) with a certain recognition ability; immobilized on macroporous cryogel as support matrix. The target molecule to be isolated is selectively captured by the complementary ligand by passing the solution mixture containing the target molecule through the cryogel column under appropriate conditions (Hajizadeh et al., 2012). Large pore diameters, short diffusion paths, strong biocompatibility, flexibility, and great mechanical strength are just a few of the advantages of cryogens that have made them crucial components of bioseparation, purification and release procedures (Kirsebom et al., 2010).

In this study, epitope-imprinted cryogel discs were prepared to deveope controlled tannic acid release antimicrobial cryogel disks. pHEMA based gelatin included biocompatible cryogel discs were prepared by imprinting gallic acid unit as epitop of tannic acid. Tannic acid loaded cryogel discs were then investigated for their use as effective controlles release antimicrobial wound healing biomaterial.

2. THEORETICAL FOUNDATIONS AND LITERATURE REVIEW

2.1. Introduction to Tannic Acid

2.1.1. History of Tannic Acid

The tannic acid to which the proteins are attached was determined by Mezbaan Katzenellenbogen in 1955 by the turbidimetric procedure. Throughout this study, the pH was adjusted using HCl or NaOH. Tannic acid (TA) was routinely measured using the FolinCiocalteu reagent by Singleton and Rossi in 1965. TA and protein interact to form soluble and insoluble complexes in an experiment performed by Hrazdina et al. in 1968, and the latter

is favored by a pH close to the protein's isoelectric point and an excess of TA (Van et al., 1969). Shenai published in 1987 that TA acts as a mordant in dyeing cotton with basic dye, using the -OH group to make H-bonds with cellulose, and that it reacts with the -COOH group of basic dye (Shenai, 1987). It was published by G.K.Lopes et al in 1999 that TA has unique properties such as anti-cancer, anti-mutation and antioxidant activity (Lopes, 1999).

2.1.2. Chemical and Metabolic Structure, Bioavailability, Elimination

Tannins, which are nitrogen-free, polyphenolic and amorphous compounds, can be found in various tissues of plants such as bark, wood, fruit, fruit seed, leaf, root, and plant sap, and play a role in the regulation of the development of these tissues (Cannas, 2019; Şener et al., 2000). Tannins found in large quantities in wood and bark, as well as in smaller amounts in the leaves and fruits of a variety of plants and trees, tannins are the fourth most common source of aromatic biomolecules. Since tannins are polyphenolic, they are excellent substitutes for elaborating chemicals and as the constituents of polymeric polymers. Plants that contain tannins are vital for preventing biological dangers as well as UV radiation, free radicals, and dryness. Three types of tannins are identified: complex, hydrolyzable, and condensed tannins. The core of hydrolyzable tannin molecules is a carbohydrate that has been esterified with phenolic groups like ellagic and gallic acid.

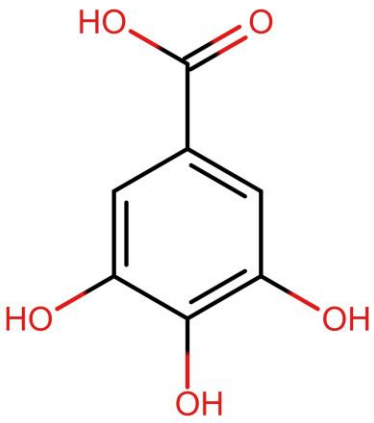

Figure 2.1. Chemical Structure of Gallic Acid

The antimicrobial action of TA; It is attributed to the inhibition of many microbial enzymes as a result of forming a complex with enzymes or substrates, the toxic effect on the membranes of microorganisms and the increase in the toxic effect of the complex formed by them with metal

ions (Goel et al., 2005). In a study investigating the antimicrobial activities of some plants containing TA, respectively; acacia bark, acorn extract, thuja powder, *Salvia Aucheri* species. *Aucheri* and *Phlomis bourgaei* extracts were the species showing the highestantimicrobial activity; it has also been reported that thuja powder and acacia bark extract, which contain high amounts of tannins, also show antifungal activity, while other extracts do not have antifungal effects (Goel et al., 2005). In 2010 Colak et al., they concluded that TA can be used as an alternative antimicrobial agent in pickling works in the leather industry. The antimicrobial effect is attributed to the interruption of cellular respiration by forming different complexes of microbial enzymes or their substrates and tannins, the destruction of electron transport systems in cell membranes, and the inactivation of essential metals due to the chelate feature of tannins. An alternate approach to prevent the production of biofilms has been investigated. The goal is to interfere with quorum sensing (QS), a signaling communication system that facilitates bacterial communication both within and between species (Ma et al., 2018). TA is a powerful QS inhibitor that also acts as an anti-biofilm drug against two clinically common pathogens that cause many persistent infections: *P. aeruginosa* (Siddiqui et al., 2015) and *S. aureus* (Lee et al., 2013). QS controls biofilm design, development, and maturation through acylated homoserine lactone (AHL), which is widely conserved in Gram-negative bacteria (Kumari et al., 2016). By focusing on short-chain AHL synthase (RhlI) to prevent QS in *P. aeruginosa*, TA inhibits the production of biofilms (Chang et al., 2014).

Additionally, TA exhibits antibacterial action against a variety of microorganisms that might lead to infections in the wounds (Bowler et al., 2001). The green one-step method yielded a three-dimensional TA-graphene composite with good antibacterial properties (Luo et al., 2015). The activity of TA against viruses is related to the inhibition of receptor binding and its effect on their activity. As it binds to the cell receptor, it prevents viruses from attaching to different surfaces. It also inhibits the binding of proteins required for metabolic processes to cells (Maginnis, 2018).

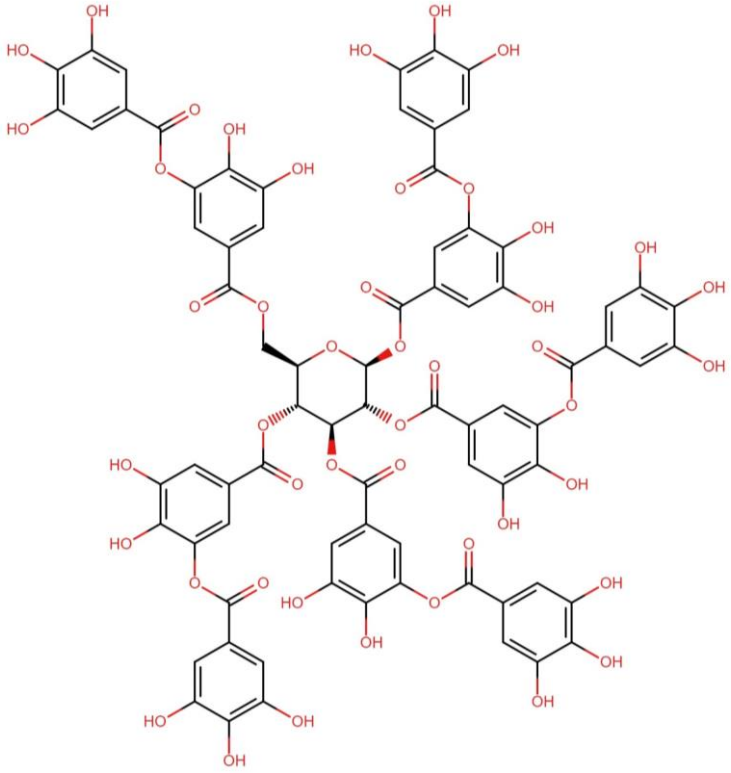

Figure 2.2. Chemical Structure of Tannic Acid

As the name suggests, they can produce carbohydrates and phenolic acids when weak acids or bases hydrolyze them. The most prevalent hydrolyzable tannin is TA. The leather tanning business is the primary use for hydrolyzable tannins, which also have antibacterial properties (Shirmohammadli et al., 2018). They do, however, show a low degree of nucleophilicity and phenol substitution, and the extraction methods can alter their macromolecular structure. Less than 10% of commercial tannins produced worldwide are hydrolysable tannins, which are also more expensive (Shirmohammadli et al., 2018). Condensed tannins are another species of tannins; because of their greater chemical reactivity, they account for more than 90% of the production of commercial tannins globally (Shirmohammadli et al., 2018). Polyhydroxy flavan-3-ols or flavan-3,4-diols (leucoanthocyanidin) are the precursors of condensed tannins, sometimes referred to as proanthocyanidins and polyflavonoid tannins, which include procyanidins, profisetinidins, profisetinidins, and prorobinetidins (Shirmohammadi et al., 2018). The majority of them are soluble in water, although they are not cleaved by hydrolysis. Finally, there are complex tannins, which are made up of both flavonoid and ellagitannin units.

However, because of their relatively low quantity and intricate structure, they have limited applicability.

2.2. Bacteria

Bacteria can be divided into two large groups, Gram-positive and Gram-negative, on the basis of a differential staining technique called the Gram stain. The Gram-positive cell wall consists primarily of a single type of molecule, whereas the Gram-negative cell wall is a multilayered structure and quite complex (Azam et al., 2012). Most microorganisms that are part of the commensal microbiota are found on the skin and in the gastrointestinal tract. The majority of such microorganisms are bacteria that have highly specialized attachment mechanisms and precise environmental requirements for survival. Normally, such microorganisms are harmless, but they may cause disease if their environmental conditions change. These opportunistic pathogens include *Escherichia coli*, *Staphylococcus aureus*, *Pseudomonas aeruginosa*, and *Bacillus cereus* (Doetsch & Cook, 2012).

The bacterial species *Escherichia* as a frequent resident of the human digestive system, *Escherichia coli* is arguably the most well-known microbiological creature. The biochemistry and genetics of *E. coli* are well understood, and the organism is still a valuable tool for fundamental biological research—many scientists even treat it like a pet in the lab. If it is found in food or drink, it is a sign of fecal contamination. *E. coli* is typically not harmful. On the other hand, some strains create enterotoxins that induce traveler's diarrhea and can occasionally cause very serious foodborne illness. It can also cause urinary tract infections. There has been evidence linking a recently discovered, developing pathogenic species of *E. albertii* to occasional infections in humans, birds, and calves (Gyles & Fairbrother, 2010). The nasal passages contain *S. aureus*. This bacterium can ferment the carbohydrate mannitol to produce acid and is tolerant of high salt chloride concentrations. *S. aureus* is a normal member of the human microbiome, found on the skin and in the nose. *S. aureus* is also a significant cause of healthcare-associated infections in patients. The bacterium can switch from benign member of the skin community to a disease-causing pathogen if it gains entry to the body through a wound (Foster, 2002). *Bacillus cereus* is a large, gram-positive, endospore forming bacterium that is very common in soil and vegetation and is generally considered harmless. It has, however, been

identified as the cause of outbreaks of foodborne illness. Heating the food does not always kill the spores, which germinate as the food cools (Sandle, 2014). Because competing microorganisms have been eliminated in the cooked food, *B. cereus* grows rapidly and produces toxins. Rice dishes served in Asian restaurants seem especially susceptible. *Pseudomonads* are aerobic gram-negative rods that are widespread in soil and water. Capable of surviving in any moist environment, they can grow on traces of unusual organic matter, such as soap films or cap liner adhesives used for many product containers. They are resistant to many antibiotics and disinfectants. The most prominent species is *Pseudomonas aeruginosa*, which is considered the model of an opportunistic pathogen (Holloway, 2020). *Pseudomonads* frequently cause outbreaks of *P. dermatitis*. *P. aeruginosa* produces several exotoxins that account form much of its pathogenicity. It also produces an endotoxin. *P. aeruginosa* often grows in dense biofilms that contribute to its frequent identification as a cause of healthcare-associated infections of indwelling medical tubes or devices. This bacterium is also a serious opportunistic pathogen for patients with the genetic lung disease cystic fibrosis; biofilm formation plays a prominent part in this (Borriello et al., 2004). *P. aeruginosa* is also a very common and serious opportunistic pathogen in burn patients, particularly those with second- and third-degree burns. Infection may produce bluegreen pus, whose color is caused by the bacterial pigment pyocyanin. Of concern in many hospitals is the ease with which *P. aeruginosa* grows in flower vases, mop water, and even dilute disinfectants (Holloway, 2020).

2.3. Antimicrobial Agents and Their Mechanisms

Antimicrobial agents are chemical biological compounds used to kill microorganisms that cause infection, reduce their effects or prevent their proliferation. It is effective against a variety of pathogens, including viruses, bacteria, fungi, as well as various other microorganisms (Kenawy, 2001). Antimicrobial agents are the general term used for substances that are both chemotherapeutic and antibiotic. Antibiotics are substances obtained by some bacteria and fungi by synthetic or semi-synthetic methods, which are lethal for other microorganisms or inhibit their growth. Chemoteratopics, on the other hand, are chemical substances synthesized by synthetic means that have a similar function to antibiotics (Finch, 2007; Jiménez-Mejías et al., 1997)

2.3.1 Chemical and Metabolic Structure, Bioavailability, Elimination

Antimicrobial polymers are polymeric materials that prevent the growth and reproduction of microorganisms such as bacteria, viruses and fungi. These materials have gained importance due to the increase in resistance to antibiotics and the inadequacy of traditional methods used to prevent infections of microorganisms (Huang et al., 2016).

Antimicrobial polymers can be obtained through chemical modifications of natural or synthetic polymers. These modifications can be accomplished by methods such as adding antimicrobial compounds to the surface of the polymers or forming functional groups within the polymer that act as antimicrobial (Jain et al., 2014; Palza, 2015).

The working mechanisms of antimicrobial polymers take place by targeting the cell wall of microorganisms or by influencing metabolic processes within the cell. These polymers interact with the lipids in the cell membrane, disrupting the structure of the membrane and causing cell death by disrupting the integrity of the cell membrane. In addition, some antimicrobial polymers inhibit the proliferation and growth of microorganisms by affecting metabolic processes within the cell (Gleckman, 2001; Jain et al., 2014; Lode, 2009).

Antimicrobial polymers can be used in many areas such as medical devices, food packaging materials, hygienic products and water treatment systems. These polymers can be useful in many areas, such as preventing nosocomial infections, controlling foodborne illness, and sanitizing water supplies (Zikmanis et al., 2021).

2.4. Molecular Imprinting Technology

The concept of molecular imprinting is very old, and the first time it revealed the famous "Key-Lock" model, which introduced the 1894 Fischer enzyme-substrate interaction, modern ideas about the issue began to emerge. In 1931, Polyakov obtained a rigid matrix as a result of the acid-drying of sodium silicate solution and the drying of gel-like silica polymer, and studied its effect on porous structure in benzene, toluene, xylene during the drying period. In 1931 Polyakov reported some unusual adsorption properties in silica particles prepared using a novel synthesis procedure (Polyakov, 1931). The first examples of molecular imprinting are synthetic organic polymers, independently presented by Takagashi, Klotz, Wulff, and Sarhan in 1972 (Takagishi & Klotz, 1972; Wulff & Sarhan, 1972). In the study conducted by K. Mosbach and

his group in 1990, MIPs based on acrylate were synthesized using amino acid derivatives and obtained positive results for their use in HPLC (Anderson & Klaus, 1990).

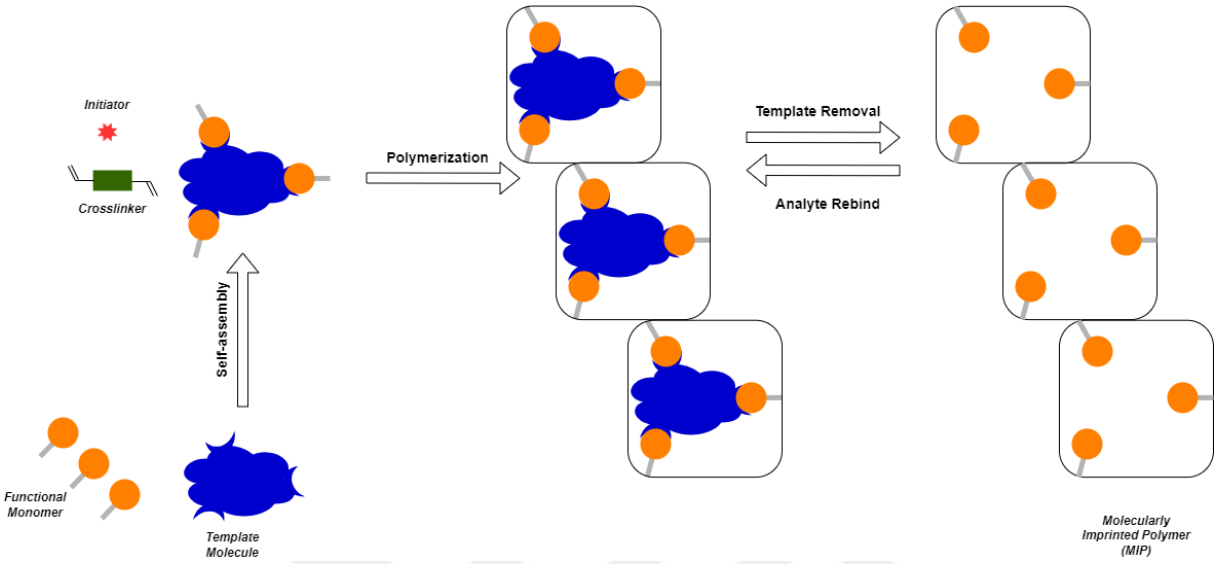

Figure 2.3. General scheme of the MIP process

It is a method for developing smart polymers with high selectivity. The template molecule forms a complex with the monomers through covalent, non-covalent or semi-covalent interactions, and memory imprinting is achieved by polymerization. With the removal of the imprinted molecule after the process, regions in the form of cavities specific to the imprinted molecule in the polymeric structure are formed. These molecularly imprinted polymers are used as an ideal material for processes such as separation, chemical determination and catalysis. In addition, molecularly imprinted polymers have been the focus of attention of researchers with their properties such as affinity, selectivity and stability, easy synthesis and easy adaptation to various applications, which are similar to natural receptors. The obtained molecularly imprinted polymers are more durable and cheaper than natural biological structures. Molecularly imprinted polymers have two most important properties, such as recognizing and binding specific molecules in biological receptors (BelBruno, 2018).

Molecularly imprinted polymers can also be used in the pharmaceutical industry to obtain purer drugs. This kind of purity is especially important when there are two mirror-image forms of the drug molecule, one beneficial and the other harmful.

Methods based on molecularly imprinted polymers are more effective for detecting and removing undesired molecules. Because each shape will fit only in the appropriate space. Thanks to this ability of molecularly imprinted polymers, sensor components are being developed for the diagnosis of toxins and pathogens (disease-causing agents) in terrorism and unknown diseases. Molecularly imprinted polymers differ from biological receptors because polymers are large and insoluble due to the high cross-linkers they contain. Biological receptors are small, flexible, and soluble. Biological molecules have very few binding sites. MIPs, on the other hand, are more suitable for most studies, as they will increase the functional binding capacity by carrying thousands of binding points (García-Domínguez et al., 2019; Kueseng et al., 2009).

The most important limitation in this regard is the requirement that the molecule to be imprinted must be small. It is imperative that the imprinted molecule be small enough to pass through the pores of the polymer, as the imprinted molecule then has to be removed from the polymeric structure. Molecules that have been imprinted so far include various drugs, hormones, proteins, amino acids, carbohydrates, dyes, pesticides, nucleotides, coenzymes, and steroids such as cholesterol.

Epitope imprinting is a spesific area of molecular imprinting technology, focused on creating polymer matrices that can specifically recognize and bind to epitopes. An epitope, often referred to as a specific part of a molecule. The epitope imprinting represents a significant advance in molecular imprinting technology. It is an advanced molecular technique that addresses challenges in molecular complexity and high costs of traditional methods. These polymers offer high specificity and selectivity for target epitopes, making them valuable in biosensing, drug delivery, and biochemical research.

Table 2.1. Molecules imprinted by molecular imprinting method and their application areas

Classification	Compound	Binding type	Application areas	References
Hormones	Enkephalin	Non-covalent	Chiral Separation	*García-Domínguez et al., 2019*
Insecticide	Atrazine	Non-covalent	Immunoassay/ Separation	*Kueseng et al., 2009*
Proteins	Transferrin	Covalent	Separation/ Purification	*Rabieizadeh et al., 2014*
Amino acids	Dansyl-Phe-Oh	Non-covalent	Sensor	*Lalo et al., 2010*
Coenzymes	Pyridoxal	Non-covalent	Catalyst	*Piletsky et al., 2001*

2.4.1. Basic Principles In Molecular Imprinting

Molecularly imprinted polymers are prepared by co-polymerization of cross-linking monomers and a complex which is pre-formed between the template molecule and functional monomers using covalent, non-covalent or semi-covalent interactions.

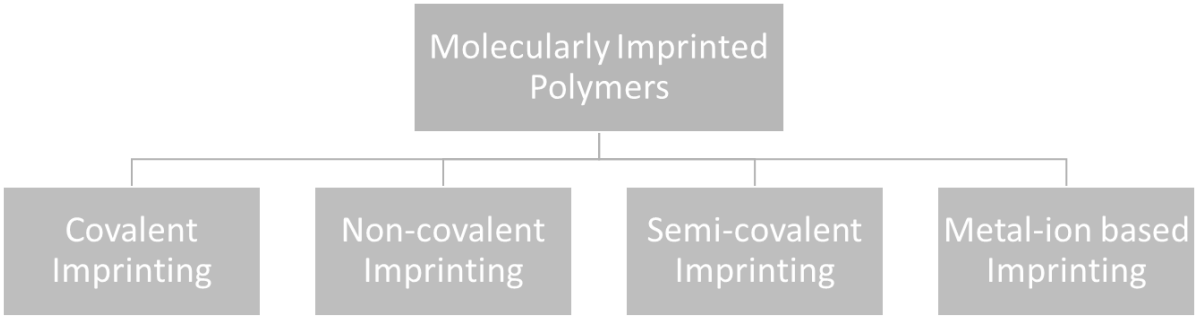

Figure 2.4. Fundamental interactions in molecular imprinting

In covalent imprinting, before the polymerization process, the functional monomer and the template molecule are linked by covalent bonds. After the polymerization process, the covalent bonds are broken and removed from the polymer to form a mold. The same covalent bond is re-formed when the template molecule is interacted with the imprinted polymers (Shea & Doughertly, 1986; Molinelli, 2004).

In non-covalent imprinting, the binding of the functional monomer and the template molecule occurs through noncovalent interactions. After polymerization, the template molecule is removed from the polymer with suitable solvents. Imprinted polymers with template molecules are bonded by non-covalent interactions (Nishide et al., 1977; Ersöz et al., 2006).

Semi-covalent imprinting; the template molecule, which can make covalent or partial covalent bonds, polymerizes by forming non-covalent bonds with the monomer mixture. The template molecule is removed from the environment by hydrolysis. With the removal of the template molecule, the functional regions are uniformly distributed throughout the polymer. Backlinking of the template molecule is based on noncovalent interactions and there is no kinetic hindrance other than diffusion (Bystrom et al., 1993; Sellergren et al., 1990).

In metal-ion imprinted polymer synthesis, metal ions are used either directly themselves or as complexes of metal ions as template molecules. In polymers where metal ions are template molecules, the pre-polymer complex is cross-linked with metal-binding ligands and polymerization of specific metal complexes is carried out together with functional monomers

on the surface of the emulsion drop. In the crystal imprinting method, recognition occurs as a result of interaction with metal ions on the surface of the crystal (Işıkber & Baylav, 2018).

2.4.2. Fundamental Components of Molecular Imprinting

The template molecule plays a key role in the success of imprinting in all molecular imprinting processes. However, not all template molecules may be suitable for direct templates for various reasons. Alternative imprinting strategies may arise in cases where the template molecule undergoes different reactions or is unstable under polymerization conditions for any reason (Kuwata et al., 2015). Another limitation of the template molecule is the molecule size. Small molecules are generally preferred as templates in the molecular imprinting process since it will be difficult to remove very large molecules from the cross-links of the polymer. However, with newly developed methods, it can be imprinted on large molecules. Functional monomers are responsible for binding interactions at imprinted recognition centers. Where more than one monomer is used together, (Kuwata et al., 2015) it is necessary to ensure that the reactivity ratios of the monomers support copolymerization.

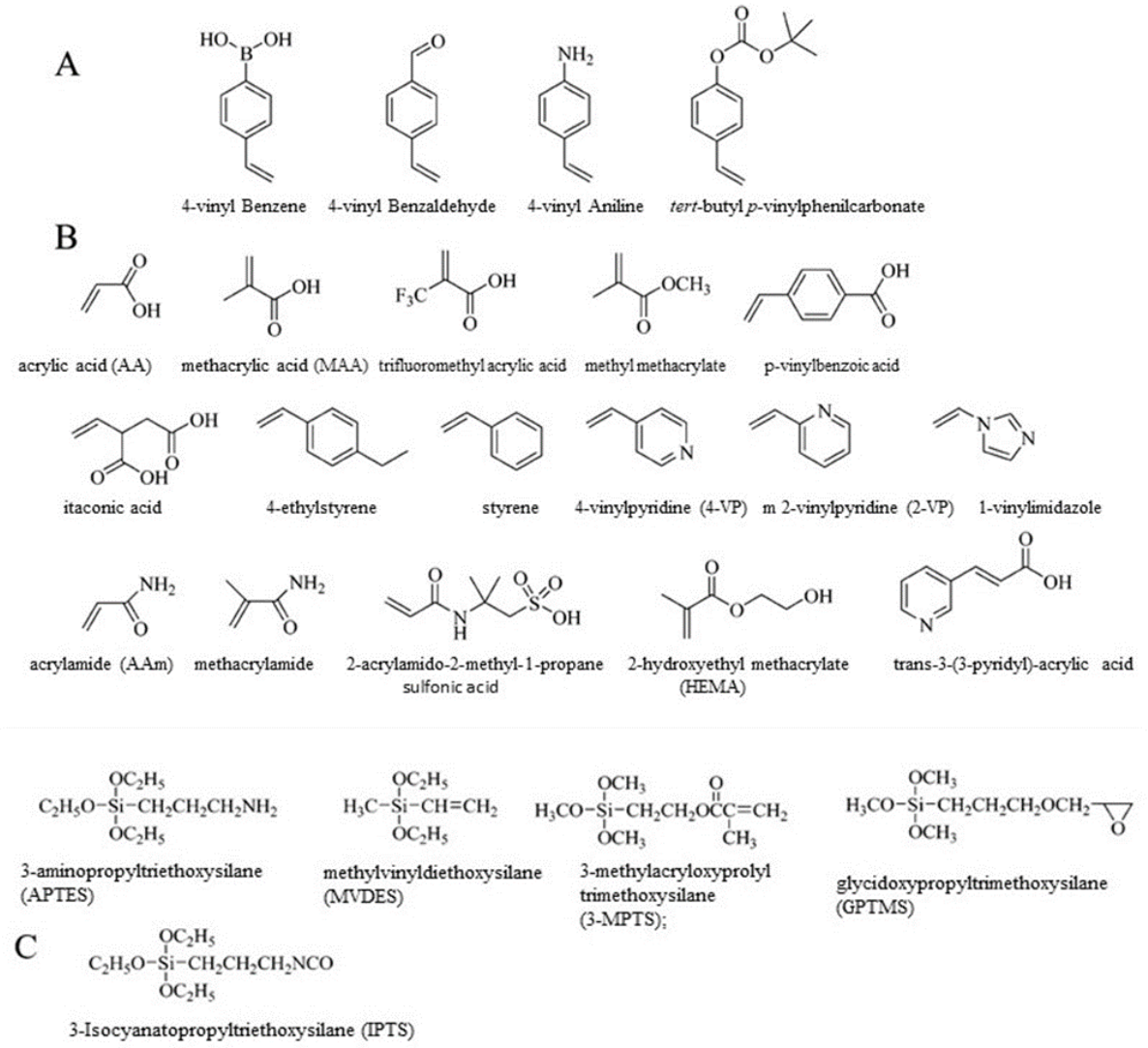

Figure 2.5. Major functional monomers used in molecular imprinting (A) Covalent Functional monomer (B) Non-covalent Functional monomer (C) Semi-covalent Functional monomer.

First, the cross-linker controls the matrix structure of the polymer, so the polymer can be in gel form, macroporous, or microgel powder form. Finally, the crosslinker determines the stability of the polymer matrix. In molecular imprinting processes, it is generally preferred in terms of obtaining macroporous and mechanically resistant materials, as well as increasing the stability of the recognition centers of highly crosslinked, imprinted polymers. For this reason, molecularly imprinted polymers generally contain over 80% crosslinker (Gönen, 2006). Otherwise, the functional monomer or cross-linking agent may polymerize more dominantly

and copolymerization may not be successful. Another important parameter is the mole percent ratio of the crosslinking agent to the functional monomer. At excessively high mole ratios, the crosslinking agent may interact with the functional monomers or template molecule by non-covalent interactions, reducing the effect of molecular imprinting (Gönen, 2006).

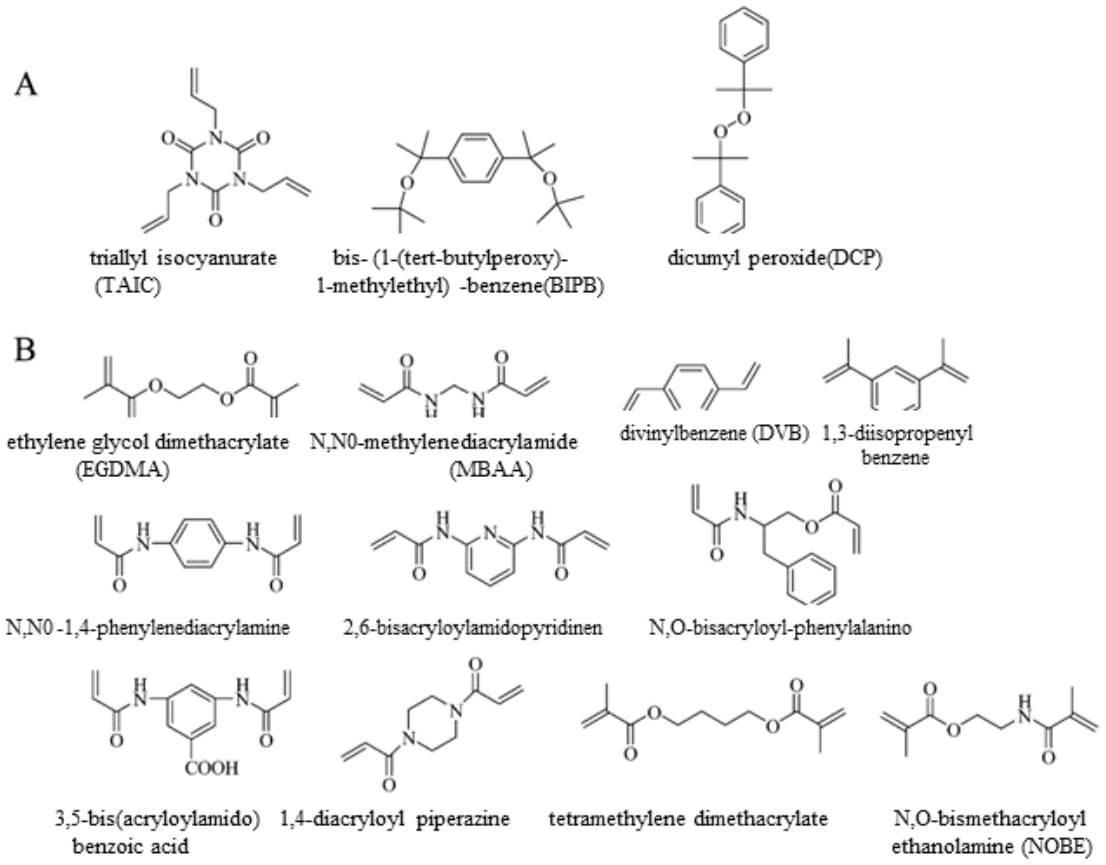

Figure 2.6. Major cross linkers used in molecular imprinting (A: covalent cross linkers, B: non-covalent cross linkers)

The word "porogen" is often used instead of the word "solvent". During polymerization, solvent molecules are dispersed in the polymer structure and after polymerization, pores are formed in the polymer structure with the removal of the solvent. The use of solvents with good thermodynamic properties results in uniform pore formation and high specific surface area formation, whereas thermodynamically poor solvents result in uneven pore formation and low

specific surface area formation. In covalent imprinting, many solvents can be used if they dissolve the components in the desired manner.

Neverthless in non-covalent imprinting processes, the interaction between solvent, template and functional monomer plays a critical role in complex formation. The best solvents are those with low dielectric constants such as toluene and dichloromethane. On the other hand, the average pore diameter of the prepared polymer also depends on the type of solvent.

Many chemical initiators with different chemical properties are used as radical sources in free radical polymerization. Initiators are used in relatively small amounts (approximately 1%) compared to monomers (Yan & Row, 2006).

Table 2.2. Chemical structures of common initiators used in molecular imprinting

Initiator	**Chemical Structures of Initiator**
2,2'-azobis(isobutyronitrile) AIBN	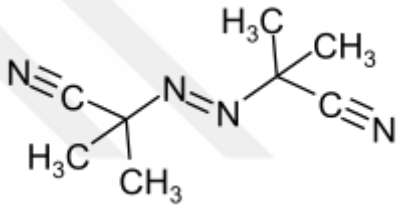
Azobis Dimethyl Valeronitrile ABDV	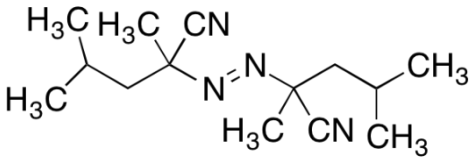
Benzoylperoxide	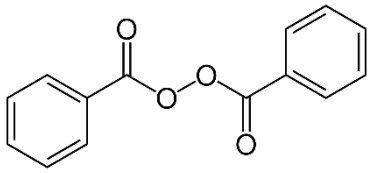
4,4'-azo(4-cyanovaleric acid)	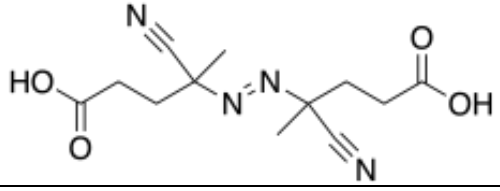

2.5. Cryogels and Usage Areas of Cryogels

Cryogels (from the Greek word kryos, meaning ice) (Lozinsky, 2002) were first reported about 50 years ago, and these polymer gels have attracted a lot of attention for their highly unusual properties. It is a specific type of gelation that occurs. This technique was used by Lozinsky and his research group to obtain a macroporous polymeric gel. Cryogels are heterogeneous open-pore structures synthesized in semi-frozen aqueous media and show high mechanical strength and elasticity. However, the adsorption capacity of cryogels is low due to their large pore structure (Kwon et al., 2008; Petrov et al., 2011; Bereli et al., 2010). Cryogels are very resistant. Cryogels can be compressed without cracking in their microstructure. This feature is due to the high cross-linking and network structure with thick pore walls. (Dinu et al., 2007). Therefore, the cryogel structure is more resistant to deformation. Cryogelation makes it possible to obtain structures with different morphologies compared to gels synthesized in non-frozen systems. In order to synthesize reproducible structures, all experimental polymerization parameters must be carried out in a controlled manner. Freezing temperature and speed, monomer composition and concentration, solvent selection, thermal history of the reaction mixture, gelling agent, etc. parameters determine the formation of cryogen structuring in the polymeric gel system (Plieva et al., 2010). Cryogels are a type of hydrogel that are prepared by freezing a polymer solution followed by lyophilization, resulting in highly porous and 3D network structure. They have a range of potential applications, including biomedical applications, environmental applications, sensing applications, energy applications, drug delivery applications. Biomedical applications benefit significantly from cryogels, employing them as scaffolds in cell culture and tissue engineering. This is attributed to cryogels' biocompatibility and expansive surface area. In environmental contexts, cryogels play a pivotal role in water purification, oil spill cleanup, and the removal of heavy metal ions from wastewater. Their high porosity and effective adsorption properties make them indispensable in sensing applications, functioning as platforms for detecting a diverse range of chemicals and biological molecules. In the realm of energy applications, cryogels find utility as catalysts and contribute to fuel cell technology, leveraging their remarkable surface area and conductivity. Furthermore, cryogels are instrumental in drug delivery applications, serving as carriers for

controlled drug release. Their high porosity, capacity to encapsulate drugs, and controlled release properties make them valuable in this domain.

2.6. Antimicrobial Applications of Cryogels

Utilizing macroporous materials to support biomaterials, such as cells, enzymes, and the like, and then applying them to water treatment is one of the most intriguing areas of research. These applications are intriguing because cryogels' porous structure is crucial for microbial development and provides better properties than other commercial hydrogels used for cell entrapment, such as unrestricted mass transfer of substrates and metabolites (Lozinsky & Plieva, 1998). Many pollutants have been investigated. For instance, the degradation of polycyclic aromatic hydrocarbons (PAHs) in water using Rhodococcus cells as a biocatalyst has been shown in a fluidized-bed bioreactor using cryogel carriers (pVA and pAAm) in addition to a carrier based on sawdust (Kuyukina et al., 2009). The increased cell entrapment reported for these materials was due to their improved catalytic activity and consequent oxidation of PAHs by sawdust-based carrier.

PVA cryogels have been shown to be effective for denitrification processes and have been used extensively as carriers of bacteria, such as *Thiobacillus denitrificans*. The PVA-entrapped cells have been shown to remove more nitrate than the free cells (Zhang et al., 2021). Using immobilized marine sludge in PVA carriers, nitrification of ammonia-polluted seawater was investigated in addition to denitrification (Furukawa et al., 1993). In stirred tank reactors, deammonification was recently investigated using immobilized anammox sludge in PVA cryogels applied to actual (swine) wastewater. The results of the investigation may demonstrate that within a 5-month period, high clearance rates (>93%) were achieved and the immobilized bacteria developed resistance to nitrate inhibition (Magri et al., 2012)**.** Other groups have synthesized cryogels for wound healing purposes. A polysaccharide-based savlon-loaded antibacterial cryogel was reported to be effective for wound healing applications (Chhatri et al., 2011), as it was shown to possess antibacterial properties being effective against *E. coli* in vitro. This could find its use in wound dressings; however, no preclinical data are yet available.

Antibacterial cryogels, a subset of hydrogels endowed with antibacterial properties, find diverse applications across various domains. In the medical field, these cryogels serve as effective wound dressings to mitigate infection risks and also function as drug delivery systems for antibiotics. A study incorporating zinc oxide into polyvinyl alcohol-based cryogels for wound dressings revealed enhanced antibacterial activity with increased zinc oxide content, coupled with optimal water absorption up to a certain threshold (Chaturvedi et al., 2016). In the realm of food packaging, antibacterial cryogels contribute to extending the shelf life of food items by curbing bacterial growth. Their utility in water purification is evident, as they serve as filters to eliminate harmful bacteria. A study by Siew-Leng Loo et al. demonstrated the synthesis of poly sodium acrylate-based cryogels with silver nanoparticles, a potent antibacterial agent. The cryogels effectively inactivated bacterial cells within a short contact time, suggesting their potential application in water disinfection (Loo et al., 2013). Antibacterial cryogels also play a role in agriculture, where they are employed to manage plant diseases caused by bacteria. In the textile industry, the addition of antibacterial cryogels to textiles serves to inhibit bacterial growth, enhancing the hygiene and odor resistance of the fabrics. While these applications highlight the versatility of antibacterial cryogels, ongoing research in the field may unveil additional uses for this innovative material.

3. MATERIALS AND METHODS

3.1. Materials

Tannic Acid (TA), Gallic Acid (GA), 1- vinylimidazole (VIM) and glutaraldehyde were purchased from Sigma-Aldrich (St. Louis, MO, USA). 2- hydroxyethyl methacrylate (HEMA), Ethylene Glycol Dimethacrylate (EGDMA), Gelatine, ammonium persulfate (APS) and N,N,N',N'-tetramethylene diamine (TEMED) were supplied from BioRad. All other chemicals used in this study were supplied from Sigma-Aldrich (St. Louis, MO, USA). Required solutions were prepared using ultrapure Type 1 water (DI) with a conductivity of 18 MΩ-cm at room temperature and analytical grade reagents. All reagents were stored according to provided information and waste materials were disposed abiding by waste disposal regulations. Phosphate-buffered saline (PBS). Cultures of *S. aureus* (29213) and *E.coli* (25922) were obtained from American Type Culture Collection (ATCC).

Shimadzu Type ATX224 No. D307039788 Electronic Balance was used for weighing of chemicals and samples. Scientific Vortex Mixer (Daihan, Korea) was used to mix solutions. Model of Millipore DIRECT-Q®3 ultrapure (type 1) water with BioPak®ultrafiltration cartridge with Millipak®Express 20 (0.22 µm) membrane filter was used for water system. The GENESYS 150 UV-Vis Spectrophotometer (Thermo Fisher Scientific, USA) and used for quantification of TA to examine adsorption capacity, and other characterisics of obtained cryogel discs. Morphology of synthesized discs were characterized by SEM (JEOL JSM 5600, Jeol Co.,Tokyo, Japan), FTIR (Fourier Transform Infrared) spectrometer (Jasco FT/IR-6700, Japan), Hitachi HT7700, Japan. Basic laboratory equipment and consumables are not included. It has not been required to list basic laboratory equipment.

3.2. Method

3.2.1.Synthesis of epitope imprinted and non-imprinted pHEMA based cryogels

Pre-complex was formed to synthesize GA imprinted cryogels (MIP). The pre-complex was synthesized using GA:VIM at a ratio of 1:8 (mole:mole). To prepare the GA-VIM precomplex, GA (20 mg, 0.118 mmol) was dissolved in 1 mL of deionized water (DI). VIM (0.944 mmol, 689 mg) was added to this solution at room temperature. Solution was kept in the refrigerator at +4°C for 2 hours.

During the cryogel synthesis process, 0.05 g of gelatin was mixed with 13.5 mL of DI at a temperature of 45 °C, using a magnetic stirrer, for approximately 1 hour. After ensuring that it was mixed well, it was allowed to reach room temperature and pre-complex was added to the mixture. Then, monomer HEMA (1.3 mL) and EGDMA (0.506 mL) were added respectively. During the process, the cryogel was treated with ice water to prevent it from polymerizing at room temperature. Then, 25 µL glutaraldehyde (25%) was added as a crosslinker. Then, 20 mg of polymerization initiator ammonium per sulfate (APS) was added, followed by 25 µL of N,N,N',N'-tetramethylene diamine (TEMED). After the addition of TEMED, before polymerization started, the polymer material was poured into the petri dish and kept at -18 °C for 24 hours. At the end of polymerization, the cryogel was kept at 25 ^{o}C room temperature until it dissolved. After complete dissolution, it was washed with DI for approximately 1 h. By removing the materials that did not participate in polymerization, 18 mm diameter sections were

cut from the samples using a perforator to prepare them for experiments. Cryogels were kept at +4 °C in DI until they needed to be used.

The same steps were followed for the synthesis of NIP, which did not undergo molecular imprinted and will be used as a control group, without adding GA to the medium.

3.2.2. Template Removal Studies

After the washing process was completed, in order to obtain specific cavities by removing the GA template molecule from the synthesized MIP from the polymeric structure; cryogel discs were reacted with PBS (10 mM, pH 7.4) elution solution containing 0.5 M NaCl. At this stage, 35 ml of elution solution was added to the MIPs and then interacted in the rotator for 2 hours. The final solution was measured spectrophotometrically at 273 nm, and the GA template molecule was removed until GA was not detected (Zenger & Pesint, 2022).

3.2.3. Characterization Studies

3.2.3.1. Swelling Tests

The swelling behavior of cryogel discs was measured using 3 samples each of MIP and NIP cryogels. The swollen weights (swollen in DI), dry weights (lyophilized for 24 hours at 0.001 mbar and -50 °C), and squeezed weights (immersed in an absorbent surface) of each disc were measured using a precision balance. The measurements for each sample were repeated 3 times.

For swelling experiments, Polimerzation Yield (%), Swelling Ratio (%), and Macroporosity (%) were calculated. For this purpose, the weights of swollen cryogel discs that reached equilibrium swelling state by absorbing water were measured. Then, the excess water of these cryogels was squeezed on a cellulose paper and the weights of their final forms were measured. Finally, the discs were frozen and dried using a lyophilizer (Lyophilizer, BK-FD10P, Biobase, China), and the weights of the dry cryogels were measured. The total mass of the monomers

used in cryogel formation was determined (m_T). The polymerization yield (%) was calculated according to Equation 3.1 given below:

$$\text{Polymerization Yield (\%)} = (m_{dry} / m_T) \times 100 \quad (3.1)$$

Swelling ratio (%) is calculated according to Equation 3.2 given below:

$$\text{Swelling ratio \%} = [(W_s - W_0) / W_0] \times 100 \quad (3.2)$$

Where, W_0 and W_s are the weights of cryogel discs before and after swelling, respectively.

To determine the total volume of supermacropores in cryogels as a percentage, the macropore volume was calculated using the Equation 3.3 given below:

$$\text{Macroporosity (\%)} = (m_{swollen} - m_{squeezed})/m_{swollen} \times 100\% \quad (3.3)$$

3.2.3.2. Structural Analysis

MIPs and NIPs were characterized using FTIR (Jasco, FT/IR-6700, USA). For FTIR analysis, the synthesized MIPs and NIPs were placed in the device in powder form. N_2 gas was introduced into the sample chamber for 10 minutes to minimize interference from environmental gases and vapors on the sample spectrum. The spectrum was measured in the wavenumber range of 4000-400 cm^{-1}. By comparing the literature, polymer formation and the structure of the bonds were observed.

3.2.3.3. Surface Morphology

The process of SEM analysis was used to investigate the morphological structures of MIP and NIP cryogels. The samples were dried in a lyophilizer (Lyophilizer, BK-FD10P, Biobase, China) before SEM analysis. After drying, the cryogel discs samples were fixed by passing them through onto the SEM sample plate using a conductive adhesive to obtain SEM images. By coating the sample surface with gold under vacuum, the surface was made conductive and SEM images of the samples were taken at different magnifications. The SEM images showed the morphological structures of the cryogels.

3.2.4. Adsorption Studies

The specific adsorption properties of MIP and NIP for TA were studied with the batch system with TA aqueous solutions at 25 °C (at pH 7.4). The effects of equilibrium TA concentration (1.5-10 mg/mL) on TA adsorption were investigated.

MIP and NIPs were weighed equally and put into separate falcon tubes. To evaluate the effect of equilibrium TA concentration on adsorption capacity, TA solutions of various concentrations ranging from 1.5-10 mg/mL (V: 5 mL) were added onto the cryogel discs in the falcon tubes and interacted with the discs at 400 rpm at 25 °C for 2 hours. Then adsorption media were taken for spectrophotometric measurement. The amount of adsorbed TA was measured spectrophotometrically by taking absorbance values at 277 nm.

For the adsorption capacities were calculated using;

$$Q = (C_o - C_f) * (V/m) \quad (3.4)$$

Here, Q is the amount of adsorbed TA for the unit mass of discs (mg/g), C_o is concentrations of TA solutions measured before interaction with discs (mg/mL) and C_f are concentrations of TA solutions measured after interaction with discs for 2h (mg/mL), V is volume of the TA solutions (Adsorption solution) (mL), m is the dried mass of the discs (g).

Experimental adsorption data were used and adsorption isotherms were used to examine the chemical and mechanical interaction behaviors between TA molecule and cryogel discs. Langmuir and Freundlich adsorption isotherm models were used as the isotherm model in the thesis study. The suitability of the adsorption properties of TA and cryogel discs to these isotherms was evaluated. The adsorption mechanism has been explained using adsorption kinetic models.

3.2.5. Release Analyses

The study to determine the drug release kinetics was conducted for 24 hours in a rotator that operates at 20 rpm and at a constant room temperature of 25°C. In order to examine the effect of the loaded TA amount on the released TA amount; The release from cryogel discs loaded with TA at concentrations of 1.5, 3, 5, 7 and 10 mg/mL was examined separately in 10 mL DI

(pH: 7.4) medium. Samples were taken from the medium at specific time intervals, and fresh DI was added to the medium to maintain constant driving force. The released TA amount was determined using a UV-VIS spectrophotometer, and the total release values were calculated.

Each sample was measured at 277 nm in a spectrophotometer and a standard graph was created. Based on the OD values obtained according to UV-VIS spectrophotometer measurement, the cumulative release percentages of the samples were determined according to Equation 3.5 below:

$$Cumulative\ Release\ Rate\ (\%) = (\frac{The\ amount\ of\ TA, \frac{mg}{mL}}{The\ maximum\ amount\ of\ TA\ , \frac{mg}{mL}})\ x100 \qquad (3.5)$$

Here, the cumulative release rate of TA (%); It expresses the percentage of cumulative increase in the amount of TA found in samples taken at different times. The amount of TA in the sample refers to the TA concentration (mg/mL) in each sample. The maximum amount of TA in the sample refers to the maximum amount of TA that should be present in each cryogel sample (Varlık et al., 2023; Manjula et al., 2021).

3.2.6. Release Kinetics

The release processes of materials loaded into polymer materials can proceed differently (Peppas et al., 2000; Varlık et al., 2023; Çetin & Denizli, 2015). For this reason, mathematical release kinetic models have been developed for different conditions and materials.

The Korsmeyer-Peppas model is a mathematical model used to describe drug release. This model assumes that the drug release rate is dependent on the diffusion rate of drug molecules and the physical properties of the drug formulation. The Korsmeyer-Peppas model is one of the most commonly used modeling methods to characterize drug release.

The Korsmeyer-Peppas kinetic release model is expressed as follows:

$$M_t / M_\infty = k * t^n \qquad (3.6)$$

Here is represents the amount of drug released at time t, M_∞ is the total amount of drug released at infinite time, k is a constant incorporating structural and geometric characteristics of the dosage form, t is the release time, and n is the release exponent that characterizes the drug

release mechanism. This model is widely used to analyze and predict drug release behavior from various pharmaceutical formulations.

When we linearize the equation 3.6, we get the following equation:

$$\log (M_\infty / M_t) = \log(k) + n * \log(t) \quad (3.7)$$

The exponent n is determined by plotting the data from equation 3.7 on a logarithmic scale and calculating the slope using linear regression. The value of k corresponds to the intercept of this line. The value of n can be interpreted as follows (Varlık et al., 2023):

• n = 0.5: Uniform diffusion controlled by Fick's diffusion law.

• 0.5 < n < 1: Indicates a situation where a different diffusion mechanism (e.g. polymer dissolution) is in effect.

• n = 1: Pure Fick diffusion control.

• n > 1: Indicates situations where drug release is controlled by another mechanism (for example, radial diffusion).

Fickian diffusion control is typically observed in homogeneous and isotropic environments. In such cases, material transfer occurs regularly and linearly according to the concentration gradient. For instance, the diffusion of gases or small molecules is often well-described by Fick's law of diffusion (Çetin & Denizli, 2015). However, Fickian diffusion control is not always applicable, especially in complex and heterogeneous systems (such as polymer materials, gel structures) or in cases of non-Fickian Diffusion. In these situations, diffusion may need to conform to a more complex model, such as the Korsmeyer-Peppas model, rather than following Fickian principles (Peppas et al., 2000; Varlık et al., 2023).

3.2.7. Antimicrobial Studies

As part of the investigation of the antibacterial properties of the synthesized MIP and NIP cryogels, colonies were formed for the bacteria selected for use in the experiment, and then the antibacterial effects of the discs were observed. Mueller-Hinton Agar (MHA) solid medium

was prepared for antibacterial studies. *S. aureus* and *E. coli* strains were used to examine the effect of MIP and NIP discs on gram-positive and gram-negative bacteria, respectively. The McFarland standard was used to prepare bacterial suspensions. McFarland is a standard used as a turbidity standard in the preparation of microorganism suspensions. The 0.5 McFarland standard was used in this study. This standard is frequently applied during the preparation of bacterial inoculums, especially for performing antimicrobial susceptibility tests.

E. coli and *S. aureus* were prepared in PBS (pH:7.4), and their turbidity was adjusted by comparing them with McFarland 0.5 solution. After the physical evaluation was completed, the samples were checked by taking measurements at 600 nm using a UV-VIS spectrophotometer, and thus 10^8 cfu/mL bacterial inoculums were prepared. Then, 1 mL inoculum from each microorganism was taken and spread onto the MHA medium prepared in each petri dish using an L-shaped rod.

Antimicrobial analysis were carried out according to disc diffusion method. MIPs loaded with 1.5, 3, and 5 mg/mL TA were placed in the middle of MHA medium containing microorganisms. The same procedure was performed with NIPs as the control group. It was incubated at 35 ± 0.1 ºC for 24 h. According to the zones of inhibition (mm) results obtained, the antibacterial effectiveness of MIP and NIP groups on *E. coli* and *S. aureus* strains was calculated. The experiments were carried out in triplicate.

4. ANALYSIS AND DISCUSSION

4.1. Synthesis of pHEMA-based Cryogels

In the study, Cryogels without GA (NIP) to be used as a control group and GA-imprinted cryogels (MIP) were prepared, then kept at -18°C for 24 hours. Then, they were left to dissolve at room temperature. As a result of repeated experiments, it was observed that all cryogels were successfully synthesized. Then, sections with a diameter of 18 mm in the form of discs were taken from each cryogel using a perforator.

Among the successfully synthesized cryogels, MIP, which contains GA in its structure, was observed in darker yellow tones, while NIP, which is the control group, was observed in light yellow tones and a color closer to white (Fig 4.1). Only when a qualitative inference is made

can it be said that GA successfully incorporated into the structure of the cryogel. However, since both cryogels contain gelatin in their structure, their colors are in yellow tones. The appearance, elasticity and color properties of the synthesized cryogels were found to be compatible with the literature (He et al., 2021).

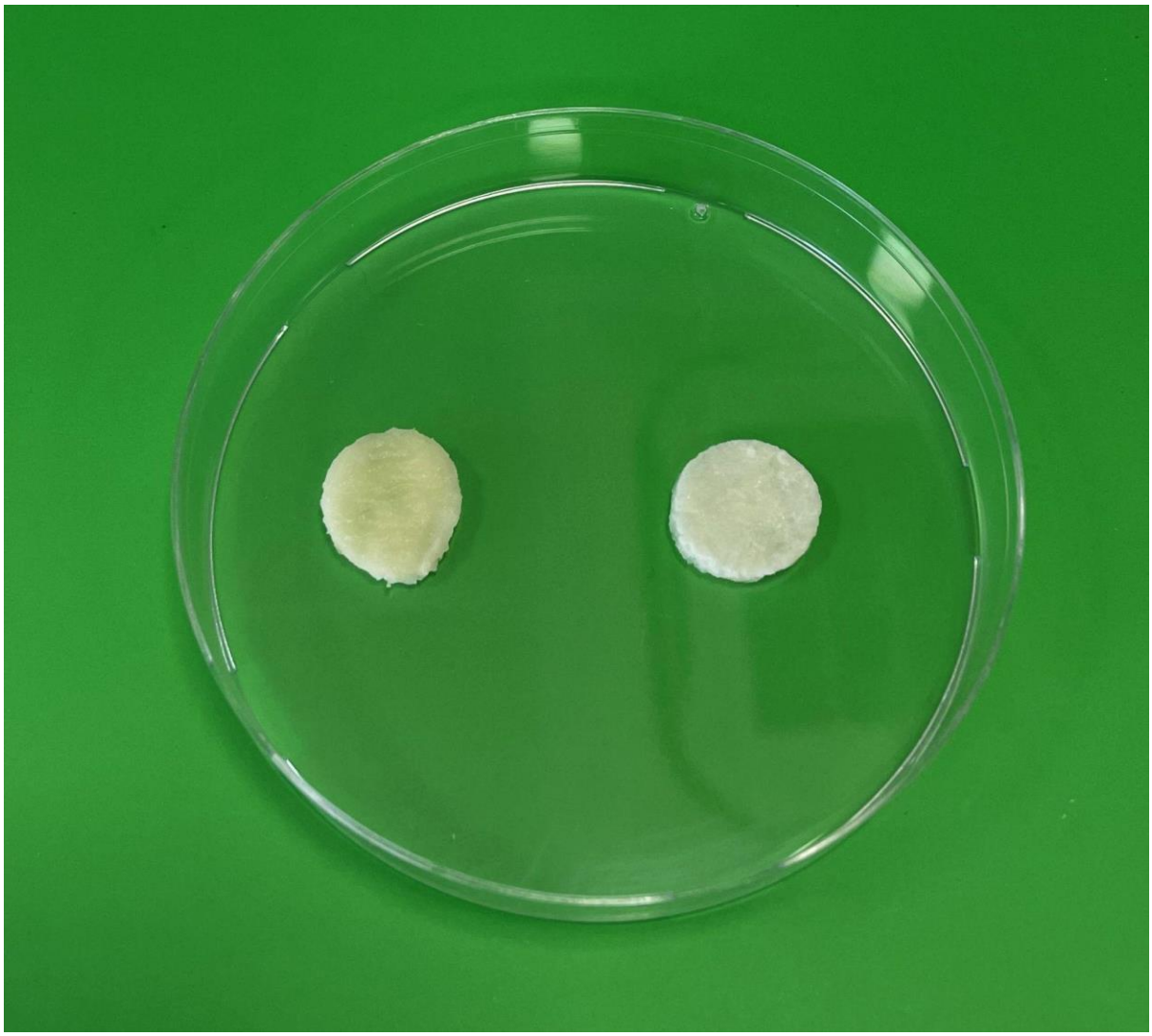

Figure 4.1. Optical photographs of MIP (left side) and NIP (right side) discs

4.2. Template Removal Studies

To obtain cavities that are specific to the template, an elution agent (0.5 M NaCl in PBS pH 7.4) was used to remove the template molecule from the MIP. After four cycles of elution, approximately 96% of GA molecules were removed from the cavities. This resulted in the formation of cavities in the structure of MIP that can selectively bind to TA.

4.3. Characterization Studies

To conduct swelling test studies, 18 mm diameter samples were taken from the swollen samples. The samples were weighed after swelling, squeezing, and drying, and the process was repeated three times. Swelling rate, porosity and polymerization yield were determined by swelling tests. When the swelling properties were examined, it was observed that the inclusion of GA in the structure reduced the gelation efficiency of the cryogel, but it did not have a negative effect on the macroporosity and swelling ratios (Table 4.1).

Table 4.1. Polymerization yield, Swelling rate and porosity of MIP and NIP

Polymers	**Polymerization Yield (%)**	**Swelling Rate (%)**	**Porosity (%)**
NIP	87	95	80
MIP	85	98	83

In this study, surface analyses were performed to observe the structural properties of cryogels and the effects of GA on the cryogel were investigated. For this purpose, SEM images of the samples were taken at different magnifications, and the sample surfaces were coated with gold under vacuum to make them conductive. Images of each cryogel sample were obtained at 1000 X, 500X and 250X magnification (Fig 4.2). When the SEM images of NIP were evaluated, it was observed that macropores were formed and cryogels were successfully synthesized (Zenger & Pesint, 2022).

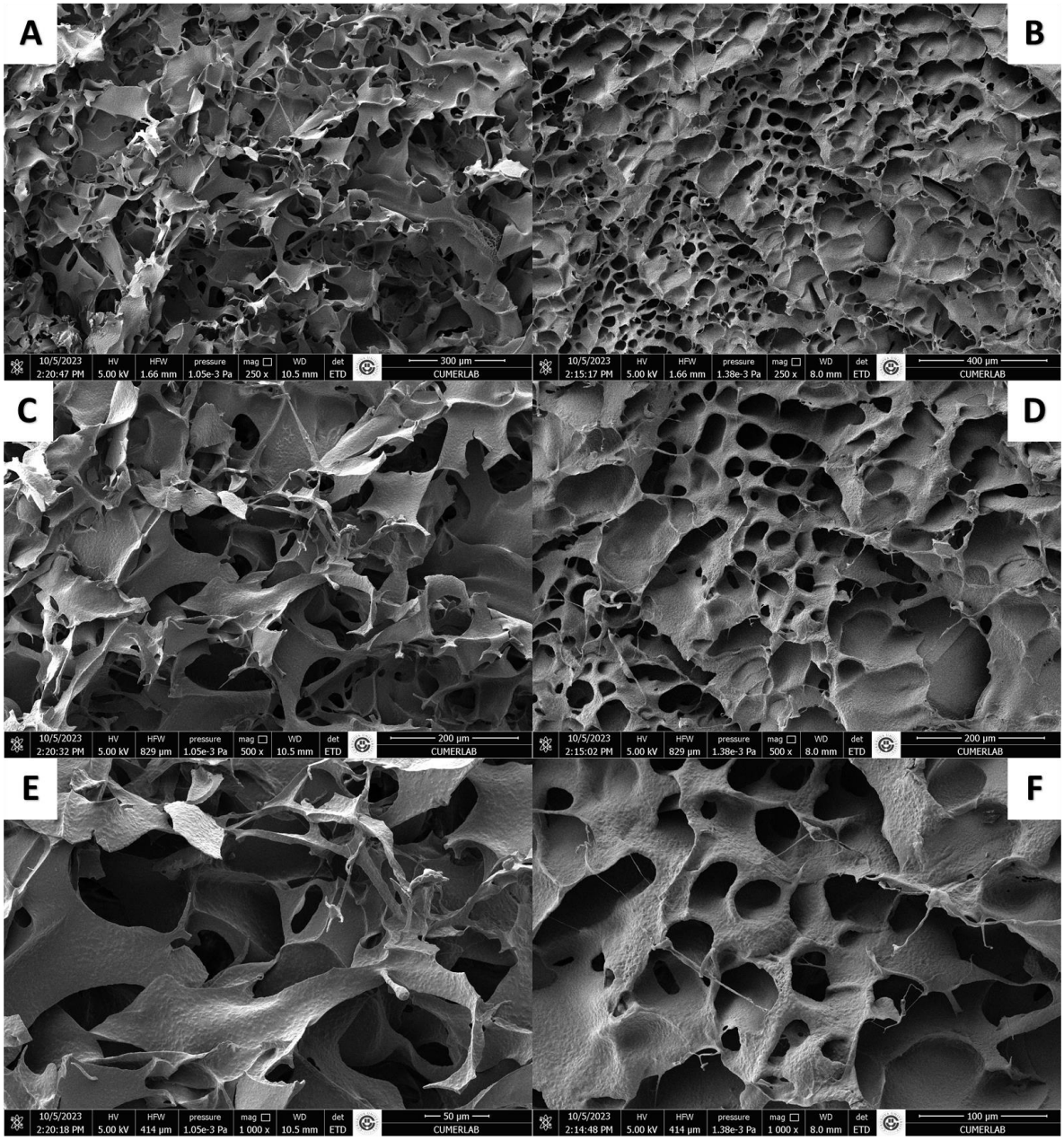

Figure 4.2. SEM images. (A) NIP, 250X; (B) MIP, 250X; (C) NIP, 500X; (D) MIP, 500X; (E) NIP, 1000X and (F) MIP, 1000X.

Structural analysis of cryogels was evaluated with FTIR-ATR results for MIP and NIP. Cryogels were analyzed without removing the imprinted molecule GA and it was shown that the GA-VIM complex entered to the MIP structure. The spectra of GA, VIM and GA-VIM precomplex (1:8) are given below, respectively (Figure 4.3.a).

When the FTIR spectrum of GA is examined, the intense peak at 3491 cm^{-1} is indicative of a robust O-H stretching vibration, pointing towards the presence of hydroxyl groups in the GA molecule. At 3266 cm^{-1}, a strong O-H stretching peak emerges, specifically attributed to the carboxylic acid group. This observation reinforces the identification of the carboxylic acid functional group within the GA. The region between 2600 and 2800 cm^{-1} displays medium-intensity peaks corresponding to C-H stretching vibrations. These peaks affirm the presence of carbon-hydrogen bonds in the compound, contributing to the overall structure of GA. The peaks at 1539 and 1604 cm^{-1} are associated with C=C stretching vibrations, characteristic of aromatic rings. These peaks serve as a distinct marker for the presence of aromatic rings within the molecular structure of GA. In the range of 1000-1300 cm^{-1}, strong peaks are observed, indicating C-O stretching vibrations. These peaks are particularly relevant to the functional groups involving oxygen atoms and contribute essential information regarding the molecular configuration of GA. Finally, the strong peaks within the 700-900 cm^{-1} range are attributed to C-H bending vibrations. These peaks emphasize the presence of carbon-hydrogen bonds and their specific bending motions within the GA molecule. In the spectrum of VIM, The peak at 3109 cm^{-1} signifies the C-H stretching of the aromatic ring, confirming the presence of the structural feature of an aromatic ring within the molecule. Medium intensity peaks around 1646 cm^{-1} predominantly represent the C=C double bonds and N-H bending associated with the aromatic ring. This indicates the distinct impact of double bonds and amine groups on the FTIR spectrum. The peaks at 1509 and 1492 cm^{-1} correspond to C-N stretching, demonstrating the presence of C-N bonds within the molecule. These peaks specifically highlight the stretching vibrations of these bonds. The peaks in the range of 1300-1400 cm^{-1} indicate strong C-N stretching vibrations within the aromatic ring. These peaks are unique to VIM and leave a prominent signature in the FTIR spectrum. When the FTIR spectrum of GA-VIM pre-complex is examined; The large peak observed at 3326 cm^{-1} is attributed to O-H stretching vibrations, believed to be associated with GA. This broadening suggests hydrogen bonding, emphasizing the interaction between GA-VIM. The peak at 1648 cm^{-1} signifies C=C stretching vibrations and N-H bending, characteristics associated with aromatic rings. This observation supports the successful inclusion of the aromatic structures from both GA and VIM in the complex. The peaks at 1503 and 1233 cm^{-1} are thought to be associated with VIM, specifically corresponding to C-N stretching vibrations within aromatic rings. This provides further evidence of the

incorporation of VIM into the complex, emphasizing the interaction between the two molecules. Additionally, the peak at 1084 cm^{-1} is attributed to C-H stretching vibrations, indicating the presence of carbon-hydrogen bonds. This observation further supports the successful formation of the preliminary complex. In conclusion, the FTIR analysis underscores the successful complexation of GA and VIM, as evidenced by the distinctive peaks associated with the individual components. The observed vibrational modes and peak patterns strongly indicate the formation of hydrogen bonds and interactions between the aromatic structures.

Below are the characteristic FTIR spectra for MIP and NIP (Figure 4.3.b). Since the structures of MIP and NIP are quite similar, their spectra also exhibit significant similarities. First of all, the wide O-H stretching band at 3376 cm^{-1} seen in both spectra is the hydrogen containing gelatin and HEMA. The C-H stretching peaks at 2948 cm^{-1} originate from the methylene groups of EGDMA and the methylene and methenyl groups of HEMA. The C=O stretching peaks at 1711 cm^{-1} represent the carboxyl or ester groups of ethylene glycol dimethacrylate and HEMA. Additionally, the C-H deformation peaks at 1450 cm^{-1} indicate the presence of methylene or methenyl groups, while the peaks at 1388 cm^{-1} and 1245 cm^{-1} reflect C-H deformations along with C-N or C-O stretching vibrations. Unlike in NIP, the band observed in MIP at 1322 cm^{-1} corresponds to amine group stretching bands, suggesting the presence of amine groups within the imprinted cavities. This observation may serve as evidence that MIP forms more hydrogen bonds than NIP. The existence of this peak can also be attributed to the inclusion of the VIM molecule in the structure. However, the frequency shift at 1711 cm^{-1}, caused by C=O vibrations, to a higher frequency in MIP, along with the difference in peak intensity compared to NIP, supports the presence of the pre-complex molecule in the structure. These variations observed in the spectra strongly indicate the incorporation of the GA-VIM pre-complex into the structure of MIP.

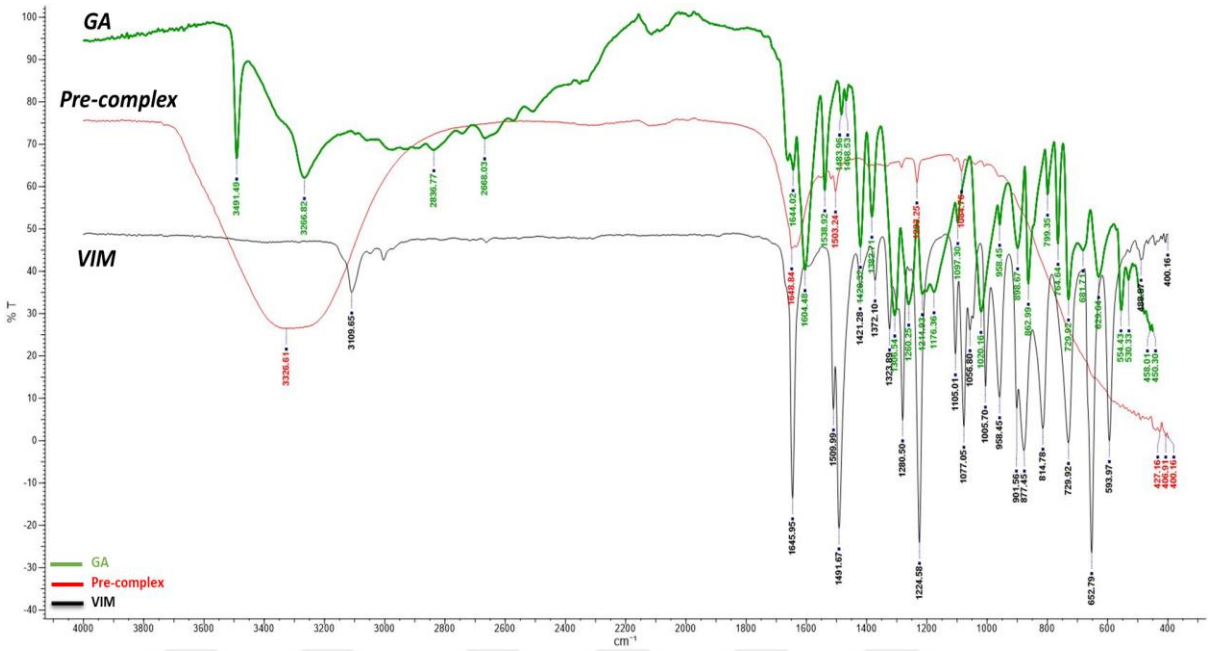

Figure 4.3.a. FTIR Spectrum of GA, VIM and 1:8 GA:VIM (n:n) pre-complex

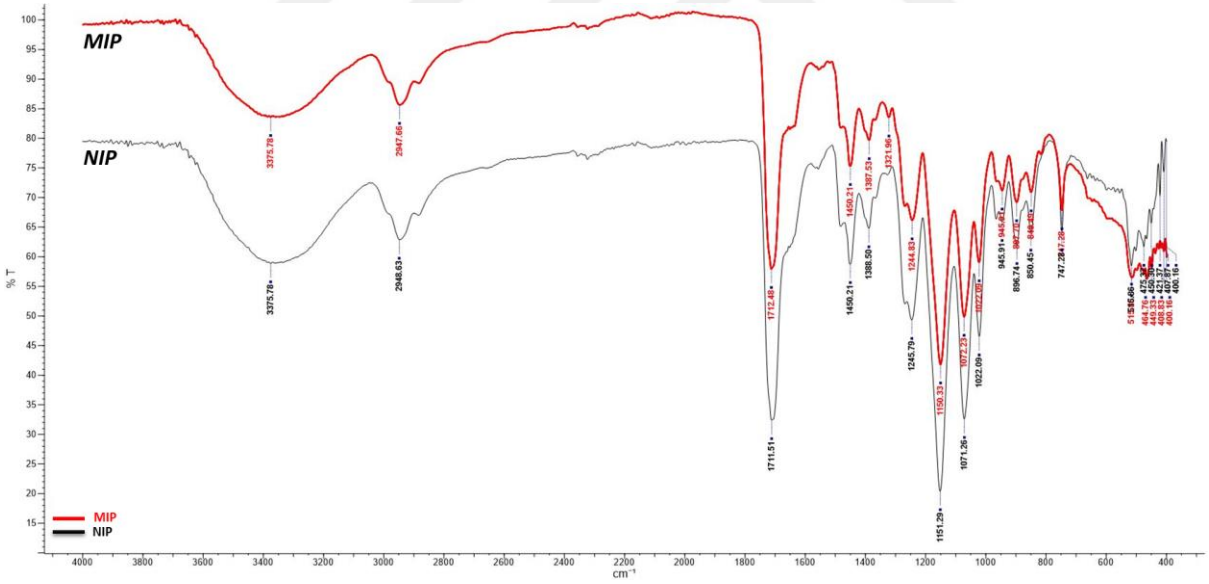

Figure 4.3.b. FTIR Spectra of MIP-HSA and NIP

4.4. Adsorption Studies

The initial TA concentration was varied in the range of 1.5-10 mg/mL and the TA adsorption capacity of the discs was examined. The maximum TA adsorption for MIP and NIP polymers was calculated as 210.27 mg and 24.74 mg per gram polymer, respectively.

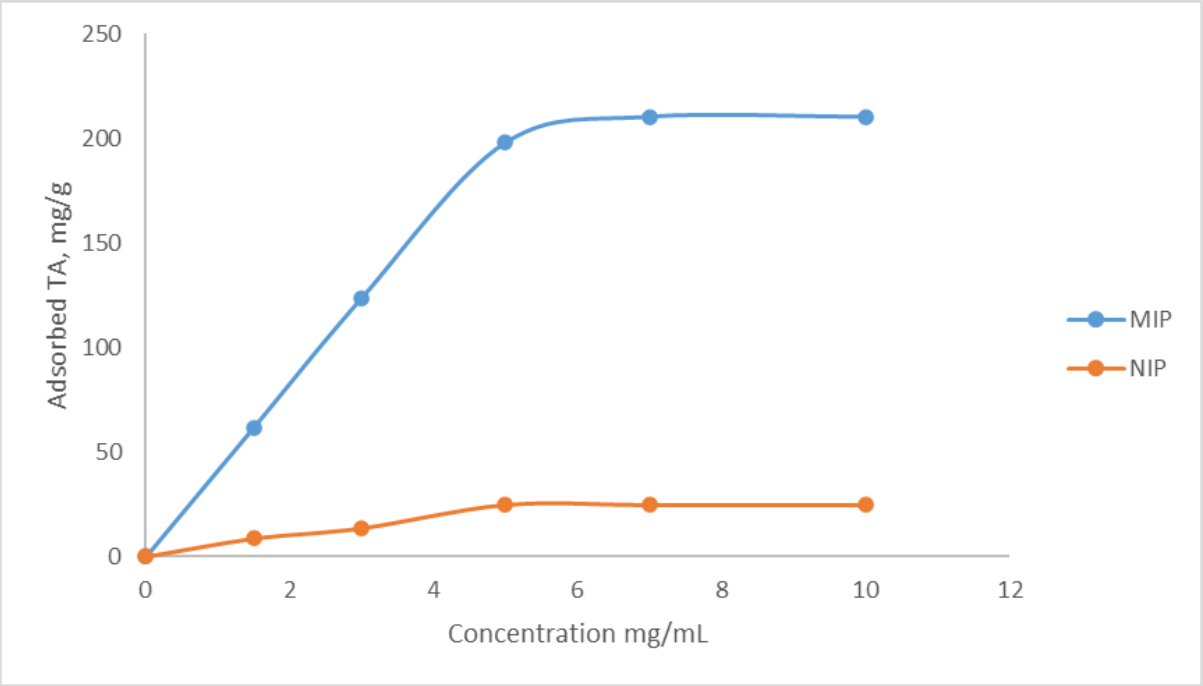

Figure 4.4. Effect of equilibrium TA concentration on TA adsorption of MIP and NIP. m_{dry}: 0.1155 g, V: 5 mL, time: 120 min, T: 25 °C, pH: 7.4, rotating: 400 rpm

The interaction behavior between adsorption isotherms and cryogel discs and TA molecules was investigated using experimental adsorption data. Adsorption isotherms reveal the relationship between the amount of adsorbate (Qe) adsorbed on the adsorbent and the equilibrium concentration (Ce) of the adsorbate in the solution (Zenger & Peşint, 2022). The Langmuir and Freundlich adsorption isotherm models were used to investigate the interaction. The Langmuir model assumes homogeneity, such as equally accessible adsorption sites, monolayer surface coverage, and no interaction between adsorbed speciess (Foo & Hameed, 2010). This model is widely used for bonding isotherms using molecularly imprinted polymers. The Langmuir model is defined by the following equation:

$$C_e/Q_e = 1/Q_{max} + 1/Q_{max}*b*C_e \quad (4.1)$$

When the equation (4.1) is linearized, the following equation is obtained:

$$C_e/Q_e = 1 / (Q_{max}.b) + (C_e/Q_{max}) \quad (4.2)$$

Here Q_e is the TA binding capacity of the adsorbent (mg/mL), C_e equilibrium concentration of TA (mg/mL), b is Langmuir constant (mL/mg), Q_{max} is the highest TA adsorption capacity (mg/g).

When C_e versus C_e/Q_e is plotted, the intersection of the line formed gives $1/Q_{max}*b$, and its slope gives $1/Q_{max}$.

Figure 4.5 shows the Langmuir adsorption isotherm of TA adsorption of MIP. The maximum TA adsorption capacity (Q_{max}) was found to be 588.23 mg/g, and the Langmuir constant (b) was 0.08 mL/mg from the slope and cut of the graph.

The Freundlich isotherm model is typically used for heterogeneous adsorption systems, unlike the Langmuir adsorption isotherm model. The Freundlich isotherm model assumes that the amount of adsorbed substance is the sum of the adsorption at all sites, and it describes reversible adsorption. Unlike the Langmuir model, the Freundlich model cannot be limited to the formation of a monolayer. According to this model, active binding sites that are close to each other interact with each other. The equation for the Freundlich adsorption isotherm is as follows:

$$Q_e = Q_f*C_e^{\,1/n} \quad (4.3)$$

When the equation (4.3) is linearized, the following equation is obtained:

$$\ln Q_e = \ln Q_f + 1/n* \ln C_e \quad (4.4)$$

Here Q_e is the amount of TA adsorbed per unit mass of adsorption at equilibrium (mg/g); C_e is the equilibrium concentration of TA in solution (mg/mL); Q_f is the relative adsorption capacity constant of the adsorbent (mg/g); 1/n is the adsorption intensity constant.

When plotting lnC_e against lnQ_e, the slope of the line formed gives 1/n, and the intersection of the line gives lnQ_f. Figure 4.6 shows the Freundlich adsorption isotherm of TA adsorption of MIP. The 1/n was found 0.6767 and the maximum TA adsorption capacity (Q_f) was found to be 53 mg/g, from the slope and cut of the graph.

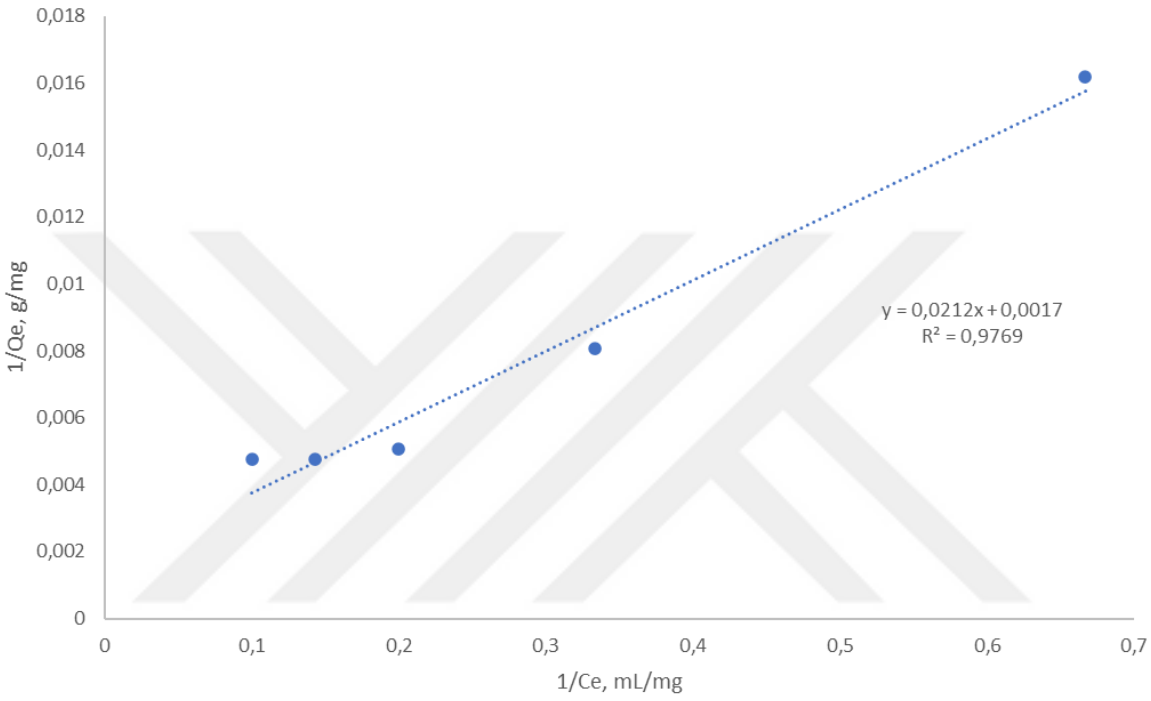

Figure 4.5. Langmuir adsorption isotherms of MIP

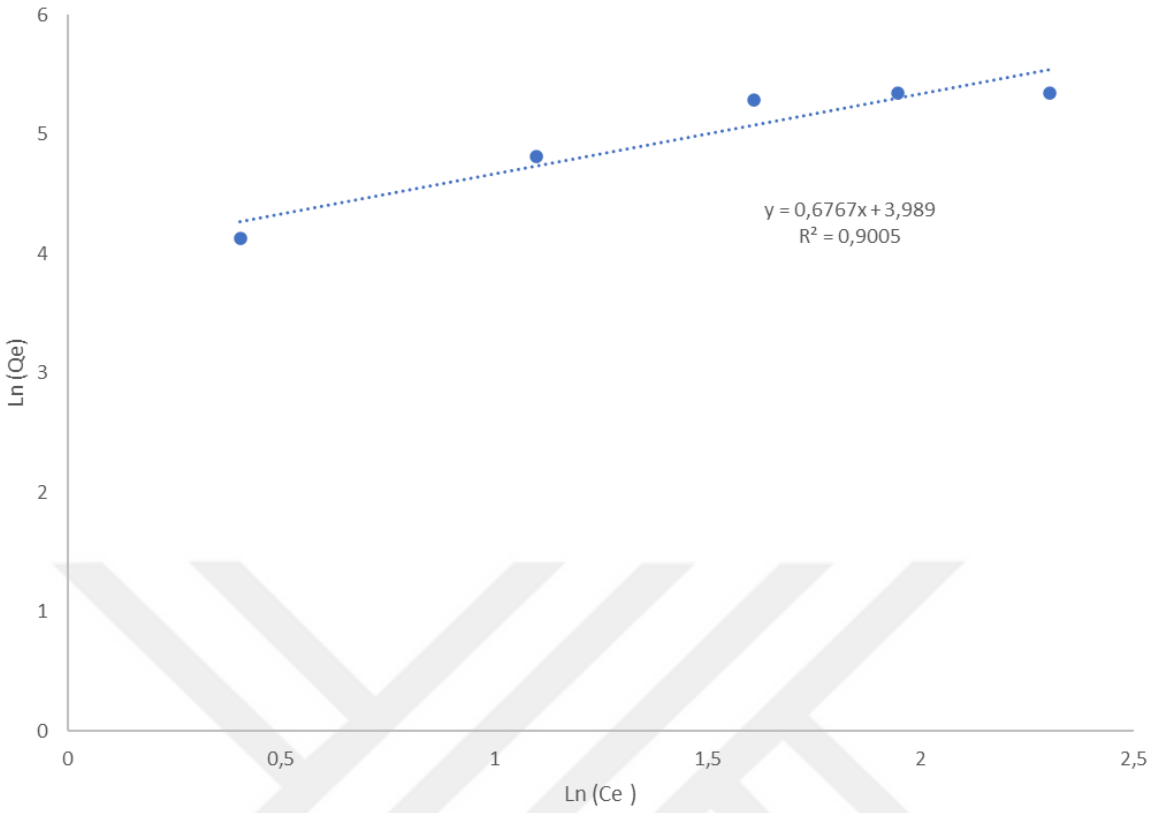

Figure 4.6. Freundlich adsorption isotherms of MIP

The study applied TA adsorption data to Langmuir and Freundlich adsorption isotherms (Fig. 4.6). The R^2 values of the graphs obtained indicated that TA adsorption conformed to the Langmuir isotherm. This result suggests that TA binding sites on the surface of prepared MIP are homogeneously distributed, monolayer, equi-energy, and with minimal lateral interaction. The results obtained from both isotherm models are presented in Table 4.2.

Table 4.2. Langmuir and Freundlich adsorption parameters of MIP

Experimental	Langmuir Constants			Freundlich Constants		
Q_e	Q_{max}	b (mL/mg)	R^2	Q_F	n	R^2
210.3	588	0.08	0.977	53.00	1.48	0.9

4.5. Release Analyses

Among the important parameters affecting the drug release rate is the amount of drug initially loaded into the polymeric system. In this study, where TA release from cryogel discs was examined, TA was loaded by adsorption at 5 different concentrations (1.5 mg/mL, 3 mg/mL, 5 mg/mL, 7 mg/mL, 10 mg/mL). In order to determine the effect of loading rate on release kinetics; Release pH (pH 7.4) and temperature (T=25^{o}C) were kept constant. When the results are examined, the release rate also increases as the initial TA loading amount increases. This is an expected result and can be explained by the increase in the driving force for the diffusion of TA from the cryogel discs as the amount of drug in the polymer system increases. When the cumulative release analysis studies of TA loaded into cryogels are evaluated, it can be concluded that the maximum release rate is reached in the first 2 hours (Figure 4.7). Based on these values, time-dependent cumulative release percentage (%) rates of each cryogel disc loaded with TA at different rates were calculated (Figure 4.8). Cryogels released almost all of the TA in their structures after 2 hours. The situation did not change in the cryogel discs with the highest TA concentration.

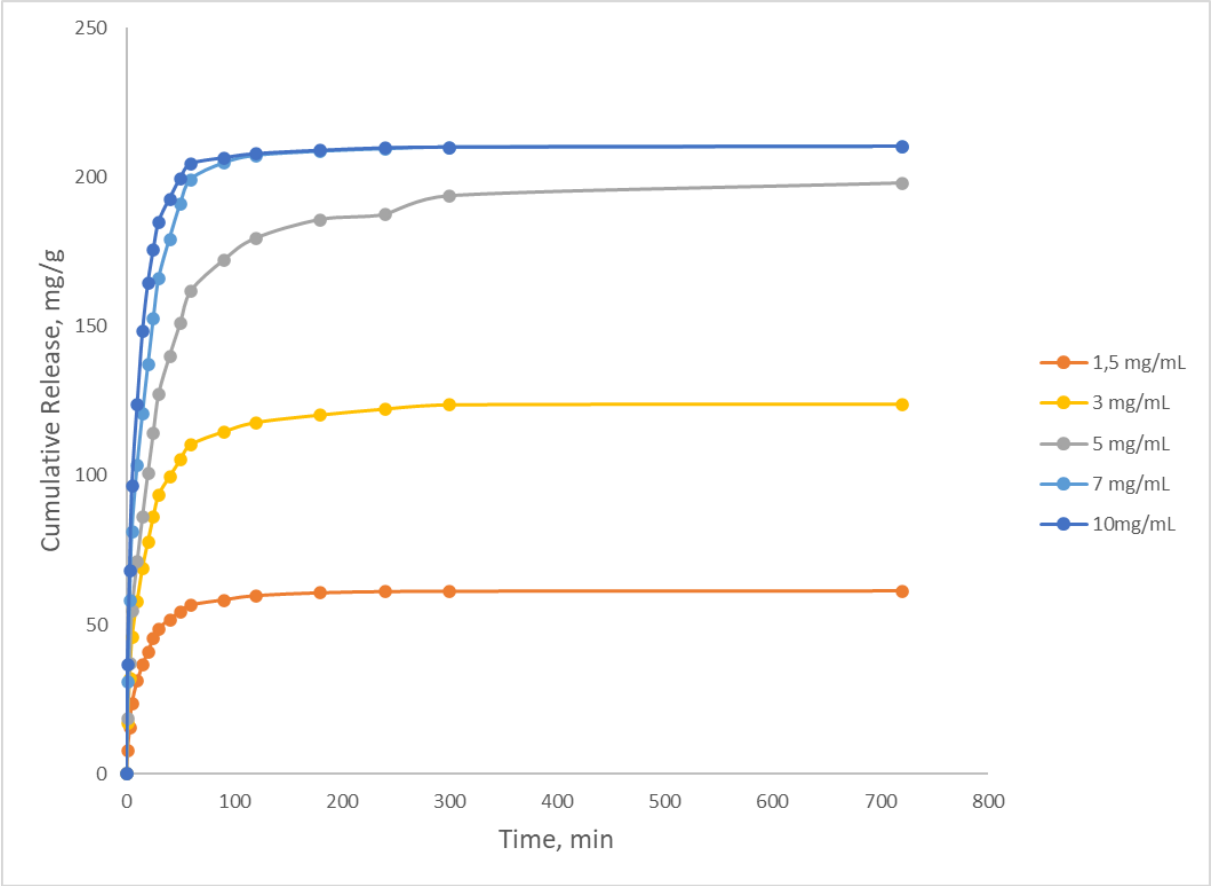

Figure 4.7. Effect of loaded TA concentration on cumulative release depending on time (T: 25 °C, pH:7.4, DI)

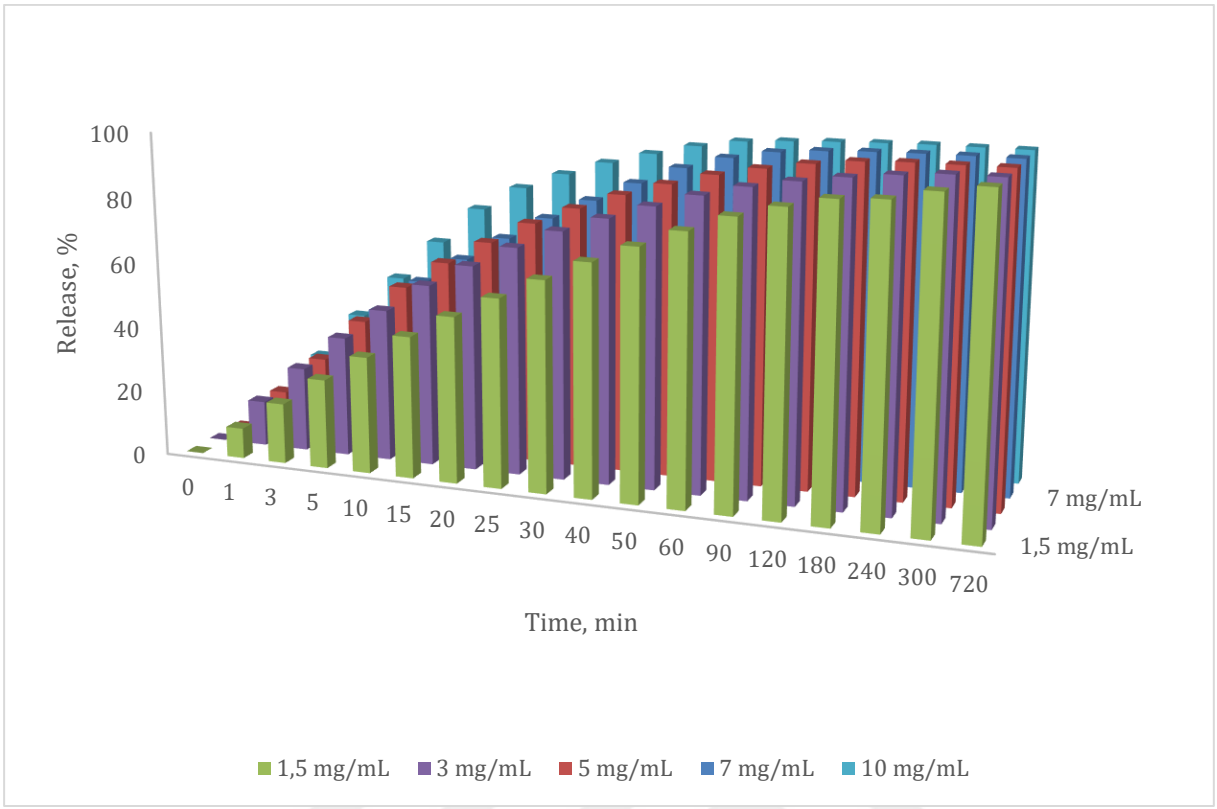

Figure 4.8. Time-dependent cumulative release rate of cryogels (%)

4.5.1. Release Kinetics

Time-dependent cumulative release rates of cryogels were evaluated with the parameters of Korsmeyer-Peppas kinetic release models (Table 4.3).

The relative effect of macromolecular relaxation on the drug release mechanism can be easily determined by modifying the experimental data to this equation. However, this equation is applicable only for the initial 60% of the total released drug.

Equation 3.6 is used to describe the general transport behavior of the solvent in the polymer and explains the type of diffusion mechanism depending on the value of n. The diffusional exponent, n, was determined by plotting the data from this equation on a logarithmic scale and calculating the slope with linear regression. Table 4.3 presents the values of n and k for release from cryogel disks containing different amounts of TA, along with regression coefficients. As clearly seen from the table, the values of n are determined to be less than 0.5. This indicates that the drug is released from the cryogel discs through a non-Fickian type of diffusion

mechanism (Çetin & Denizli, 2015). Non-Fickian diffusion is commonly observed in complex systems such as polymer materials, gel structures, or heterogeneous environments. In drug delivery systems, Non-Fickian Diffusion is an important factor for understanding and optimizing how the drug release rate changes over time (Varlık et al., 2023; Çetin & Denizli, 2015).

Table 4.3. n, k and R^2 values obtained when the Korsmeyer-Peppas release kinetics model is applied

Initial TA concentration (mg/mL)	**n**	**k**	**R^2**
1.5	0.39	1.7	0.91
3	0,38	1,7	0,93
5	0,45	2,1	0,96
7	0,37	1,64	0,93
10	0,33	1,4	0,88

4.6. Antimicrobial Studies

In this thesis, cryogel discs loaded with three different concentrations of TA showed antimicrobial activity against *S. aureus* and *E. coli*. Inhibition zone diameters of discs were determined to be larger at highest concentration of TA which is 5 mg/mL. The highest antimicrobial activity with 15 mm inhibition zone was oserved against *S. aureus*. On the other hand, inhibition zone of 12 mm was observed against *E. coli*. Antibacterial activity difference between *S.aureus* and *E.coli* is explained by cell wall structure. Because of having cell walls composed of thick peptidoglycan layer *S. aureus*, tannic acid is rapidly pass through the bacterial cell wall in comparison with *E.coli* and interfere with the internal membrane structure. When the concentration of TA increased there was no significant changes occured on the inhibition zone diameters. An inhibition zone of 12 mm was considered as an effective indicator

for strong antimicrobal activity (Mau et al., 2001). As a result, it can be concluded that TA loaded discs showed effective antimicrobial activity against both *S. aureus* and *E.coli*. According to literature, TA has been shown antimicrobial activities through various Gram-positive and Gram-negative microorganisms, such as *S. aureus*, *E. coli*, *Streptococcus pyogenes*, *Enterococcus faecalis*, *Pseudomonas aeruginosa*, *Yersinia enterocolitica*, *Listeria monocytogenes*, *Listeria innocua*, *Bacillus cereus*, *Klebsiella pneumoniae*, *Helicobacter pylori* etc. (Kaczmarek, 2020). In a study conducted by Kim et al. (2010) tannic acid samples strong antimicrobial activity on *Salmonella typhimurium* and *Enterobacter sakazakii*. The antimicrobial mechanism of TA could be iron deprivation which may work like a siderophore to chelate essential iron from the medium and make it unavailable to the microorganism (Chung et al., 1998). Moreover, Dong et al. (2017) studied the antimicrobial and antibiofilm activity of TA against *S. aureus* and concluded that antimicrobial activity of tannic acid could be attributed with the binding directly with the peptydoglycan layer of the cell wall as a result destroy its integrity. In 2019, Dabbaghi et al., studied on the synthesis of antibacterial superabsorbents based on tannic acid and resulted that the synthesized material showed antibacterial activity against both *S.aureus* and *E.coli* with being the most effective against *S. aureus* (Dabbaghi et al., 2019).

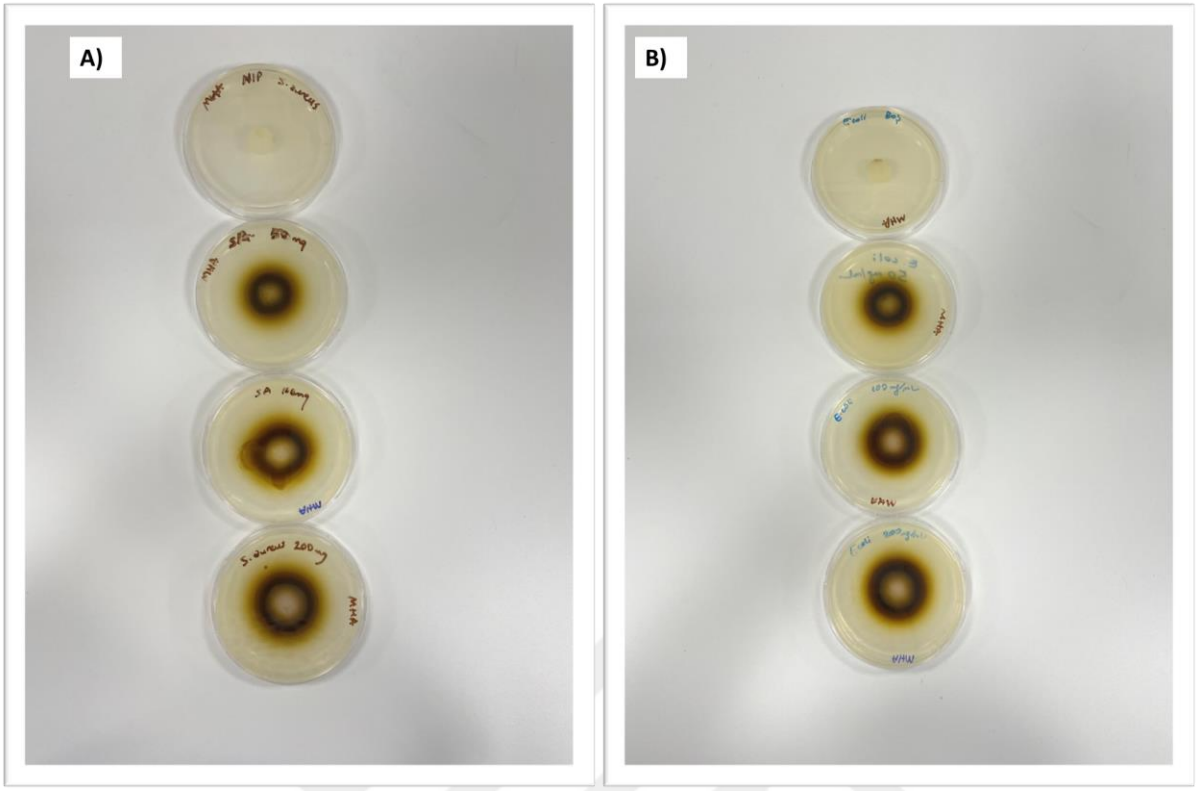

Figure 4.9. Antimicrobial results of MIPs and NIPs against; A) *S. aureus* and B) *E. coli*

5. CONCLUSIONS

Within the scope of this thesis study, epitope-imprinted pHEMA-based cryogel discs utilizing the antimicrobial effects of TA molecules and non-imprinted cryogel discs as a control group were produced. In line with this objective, GA-imprinted cryogel discs were synthesized first, and the synthesized MIPs and NIPs were characterized through FTIR, SEM, and swelling tests. Upon examination of FTIR spectra, it was observed that the pre-complex successfully incorporated into the cryogel structure. Prepared MIPs and NIPs swelled rapidly in water, reaching their final dimensions in a short time. When the equilibrium swelling and porosity ratios of the discs were examined, the ratios for MIPs were found to be higher than those for NIPs. The addition of GA to the structure is believed to increase pore formation. SEM results indicated a homogeneous distribution of the polymer matrix and cryogel discs with adequately sized pores, allowing for unobstructed release. Subsequently, GA was removed from the structure. TA loading was performed at different concentrations, and the maximum adsorption

capacity was determined to be 7 mg/mL. The release profiles of TA-loaded cryogel discs were then examined. As the TA loading rate in the polymer increased, the release rate also increased. The increase in the amount of drug in the polymer led to an increase in the driving force (concentration difference) required for the diffusion of the molecule from the cryogel disc. The increase in concentration difference resulted in an increase in the release rate. When evaluating the release kinetics, the exponent "n" indicating the type of release mechanism according to the power law was found to be less than 0.5, suggesting that the diffusion mechanism in the prepared cryogel discs is non-Fickian. From the cryogel discs placed in the reservoir, high rates of TA release occurred in the first few minutes due to the burst effect, followed by lower rates of release. After 2 hours, the amounts of released TA from the discs remained unchanged, indicating that the release was complete. Antimicrobial properties were investigated on *E.coli* and *S.aureus*, and strong antibacterial effect was observed with no significant difference between gram-positive and gram-negative bacteria.

As a result, within the scope of this thesis study, epitope-imprinted pHEMA-based cryogel discs were successfully synthesized, and the antimicrobial efficacy and release success of TA-loaded MIPs were demonstrated.

REFERENCES

Aelenei, N., Popa, M. I., Novac, O., Lisa, G., & Balaita, L. (2009). Tannic acid incorporation in chitosan-based microparticles and in vitro controlled release. *Journal of Materials Science: Materials in Medicine*, *20*, 1095-1102.

Ahmad, T. (2014). Reviewing the tannic acid mediated synthesis of metal nanoparticles. *Journal of Nanotechnology*, *2014*.

Andersson, L. I., & Mosbach, K. (1990). Enantiomeric resolution on molecularly imprinted polymers prepared with only non-covalent and non-ionic interactions. *Journal of Chromatography A*, *516*(2), 313-322.

Andrade Jr, R. G., Ginani, J. S., Lopes, G. K., Dutra, F., Alonso, A., & Hermes-Lima, M. (2006). Tannic acid inhibits in vitro iron-dependent free radical formation. *Biochimie*, *88*(9), 1287-1296.

Azam, A., Ahmed, A. S., Oves, M., Khan, M. S., Habib, S. S., & Memic, A. (2012). Antimicrobial activity of metal oxide nanoparticles against Gram-positive and Gram-negative bacteria: a comparative study. *International journal of nanomedicine*, 6003-6009.

BelBruno, J. J. (2018). Molecularly imprinted polymers. *Chemical reviews*, *119*(1), 94-119.

Bereli, N., Şener, G., Altıntaş, E. B., Yavuz, H., & Denizli, A. (2010). Poly (glycidyl methacrylate) beads embedded cryogels for pseudo-specific affinity depletion of albumin and immunoglobulin G. *Materials Science and Engineering: C*, *30*(2), 323-329.

Borriello, G., Werner, E., Roe, F., Kim, A. M., Ehrlich, G. D., & Stewart, P. S. (2004). Oxygen limitation contributes to antibiotic tolerance of Pseudomonas aeruginosa in biofilms. *Antimicrobial agents and chemotherapy*, *48*(7), 2659-2664.

Bowler, P. G., Duerden, B. I., & Armstrong, D. G. (2001). Wound microbiology and associated approaches to wound management. *Clinical microbiology reviews*, *14*(2), 244-269.

Božič, M., Gorgieva, S., & Kokol, V. (2012). Homogeneous and heterogeneous methods for laccase-mediated functionalization of chitosan by tannic acid and quercetin. *Carbohydrate polymers*, *89*(3), 854-864.

Bystroem, S. E., Boerje, A., & Akermark, B. (1993). Selective reduction of steroid 3-and 17-ketones using lithium aluminum hydride activated template polymers. *Journal of the American Chemical Society*, *115*(5), 2081-2083.

Cannas, A. (2008). Tannins: fascinating but sometimes dangerous molecules. *Cornell University, NY, USA. URL http://www. ansci. cornell. edu/plants/toxicagents/tannin. html*.

Chang, C. Y., Krishnan, T., Wang, H., Chen, Y., Yin, W. F., Chong, Y. M., ... & Chan, K. G. (2014). Non-antibiotic quorum sensing inhibitors acting against N-acyl homoserine lactone synthase as druggable target. *Scientific reports*, *4*(1), 7245.

Chaplin, A. J. (1985). Tannic acid in histology: an historical perspective. *Stain Technology*, *60*(4), 219-231.

Chaturvedi, A., Bajpai, A. K., Bajpai, J., & Singh, S. K. (2016). Evaluation of poly (vinyl alcohol) based cryogel–zinc oxide nanocomposites for possible applications as wound dressing materials. *Materials Science and Engineering: C*, *65*, 408-418.

Chhatri, A., Bajpai, J., Bajpai, A. K., Sandhu, S. S., Jain, N., & Biswas, J. (2011). Cryogenic fabrication of savlon loaded macroporous blends of alginate and polyvinyl alcohol (PVA). Swelling, deswelling and antibacterial behaviors. *Carbohydrate polymers*, *83*(2), 876-882.

Colak, S. M., Yapici, B. M., & Yapici, A. N. (2010). Determination of antimicrobial activity of tannic acid in pickling process. *Romanian Biotechnological Letters*, *15*(3), 5325-5330.

Çetin, K., & Denizli, A. (2015). 5-Fluorouracil delivery from metal-ion mediated molecularly imprinted cryogel discs. Colloids and Surfaces B: Biointerfaces, 126, 401-406.

Dabbaghi, A., Kabiri, K., Ramazani, A., Zohuriaan-Mehr, M. J., & Jahandideh, A. (2019). Synthesis of bio-based internal and external cross-linkers based on tannic acid for preparation of antibacterial superabsorbents. *Polymers for Advanced Technologies*, *30*(11), 2894-2905.

Dai, H., Abdelkefi, A., Ni, Q., & Wang, L. (2014). Modeling and identification of circular cylinder-based piezoaeroelastic energy harvesters. *Energy Procedia*, *61*, 2818-2821.

Dinu, M. V., Ozmen, M. M., Dragan, E. S., & Okay, O. (2007). Freezing as a path to build macroporous structures: superfast responsive polyacrylamide hydrogels. *Polymer*, *48*(1), 195-204.

Doetsch, R. N., & Cook, T. M. (2012). *Introduction to bacteria and their ecobiology*. Springer Science & Business Media.

Ersöz, A., Denizli, A., Özcan, A., & Say, R. (2005). Molecularly imprinted ligand-exchange recognition assay of glucose by quartz crystal microbalance. *Biosensors and Bioelectronics*, *20*(11), 2197-2202.

Finch, R. (2007). Innovation—drugs and diagnostics. *Journal of Antimicrobial Chemotherapy*, *60*(suppl_1), i79-i82.

Foster, T. J. (2002). Staphylococcus aureus. *Molecular Medical Microbiology*, 839-888.

Furukawa, Y. (1993). Depth of the decoupling plate interface and thermal structure under arcs. *Journal of Geophysical Research: Solid Earth*, *98*(B11), 20005-20013.

García-Domínguez, M., Lastra, A., Folgueras, A. R., Cernuda-Cernuda, R., Fernández-García, M. T., Hidalgo, A., ... & Baamonde, A. (2019). The chemokine CCL4 (MIP-1β) evokes antinociceptive effects in mice: a role for CD4+ lymphocytes and met-enkephalin. *Molecular Neurobiology*, *56*, 1578-1595.

Gleckman, R. (2001). What do the new antimicrobials offer? Weighing the advantages and disadvantages compared with traditional agents. *Postgraduate Medicine*, *109*(3), 87-91.

Gleckman, R. (2001). What do the new antimicrobials offer? Weighing the advantages and disadvantages compared with traditional agents. *Postgraduate Medicine*, *109*(3), 87-91.

Goel, G., Puniya, A. K., Aguilar, C. N., & Singh, K. (2005). Interaction of gut microflora with tannins in feeds. *Naturwissenschaften*, *92*, 497-503.

Gönen S, Karbonhidrat/Amino Asit Baskılanmış Akrilik Polimerlerin Hücre Biyoteknolojisindeki Kullanım Potansiyelinin Araştırılması, Yüksek Lisans Tezi, Fen Bilimler Enstitüsü, Hacettepe Üniversitesi 2006: 133

Gyles, C. L., & Fairbrother, J. M. (2010). Escherichia coli. *Pathogenesis of bacterial infections in animals*, *4*, 267-308.

Hajizadeh, S., Kirsebom, H., Leistner, A., & Mattiasson, B. (2012). Composite cryogel with immobilized concanavalin A for affinity chromatography of glycoproteins. *Journal of separation science*, *35*(21), 2978-2985.

He, Y., Wang, C., Wang, C., Xiao, Y., & Lin, W. (2021). An overview on collagen and gelatin-based cryogels: Fabrication, classification, properties and biomedical applications. Polymers, 13(14), 2299.

Holloway, B. W. (2020). Pseudomonads. In *Genetics and breeding of industrial microorganisms* (pp. 63-92). CRC Press.

Huang, G., Gao, J., Hu, Z., John, J. V. S., Ponder, B. C., & Moro, D. (2004). Controlled drug release from hydrogel nanoparticle networks. *Journal of Controlled Release*, *94*(2-3), 303-311.

Huang, K. S., Yang, C. H., Huang, S. L., Chen, C. Y., Lu, Y. Y., & Lin, Y. S. (2016). Recent advances in antimicrobial polymers: a mini-review. *International journal of molecular sciences*, *17*(9), 1578.

Işıkver, Y., & Baylav, S. (2018). Synthesis and characterization of metal ion-imprinted polymers. *Bulletin of Materials Science*, *41*, 1-11.

Jain, A., Duvvuri, L. S., Farah, S., Beyth, N., Domb, A. J., & Khan, W. (2014). Antimicrobial polymers. *Advanced healthcare materials*, *3*(12), 1969-1985.

Jain, A., Duvvuri, L. S., Farah, S., Beyth, N., Domb, A. J., & Khan, W. (2014). Antimicrobial polymers. *Advanced healthcare materials*, *3*(12), 1969-1985.

Jimenez-Mejias, M. E., Pachon, J., Becerril, B., Palomino-Nicas, J., Rodriguez-Cobacho, A., & Revuelta, M. (1997). Treatment of multidrug-resistant Acinetobacter baumannii meningitis with ampicillin/sulbactam. *Clinical infectious diseases*, *24*(5), 932-935.

Kaczmarek, B. (2020). Tannic acid with antiviral and antibacterial activity as a promising biomaterials— minireview. *Materials (Basel), 13(14)*, 3224.

Kenawy, E. R. (2001). Biologically active polymers. IV. Synthesis and antimicrobial activity of polymers containing 8-hydroxyquinoline moiety. *Journal of applied polymer science*, *82*(6), 1364-1374.

Kenawy, E. R., Worley, S. D., & Broughton, R. (2007). The chemistry and applications of antimicrobial polymers: a state-of-the-art review. *Biomacromolecules*, *8*(5), 1359-1384.

Kim, T. J., Silva, J. L., Kim, M. K., & Jung, Y. S. (2010). Enhanced antioxidant capacity and antimicrobial activity of tannic acid by thermal processing. *Food Chemistry*, *118*(3), 740-746.

Kirsebom, H., Topgaard, D., Galaev, I. Y., & Mattiasson, B. (2010). Modulating the porosity of cryogels by influencing the nonfrozen liquid phase through the addition of inert solutes. *Langmuir*, *26*(20), 16129-16133.

Kueseng, P., Noir, M. L., Mattiasson, B., Thavarungkul, P., & Kanatharana, P. (2009). Molecularly imprinted polymer for analysis of trace atrazine herbicide in water. *Journal of Environmental Science and Health Part B*, *44*(8), 772-780.

Kumari, S., Mangwani, N., & Das, S. (2016). Synergistic effect of quorum sensing genes in biofilm development and PAHs degradation by a marine bacterium. *Bioengineered*, *7*(3), 205-211.

Kuwata, T., Uchida, A., Takano, E., Kitayama, Y., & Takeuchi, T. (2015). Molecularly imprinted polymer arrays as synthetic protein chips prepared by transcription-type molecular imprinting by use of protein-immobilized dots as stamps. *Analytical chemistry*, *87*(23), 11784-11791.

Kuyukina, M. S., Ivshina, I. B., Serebrennikova, M. K., Krivorutchko, A. B., Podorozhko, E. A., Ivanov, R. V., & Lozinsky, V. I. (2009). Petroleum-contaminated water treatment in a fluidized-bed bioreactor with immobilized Rhodococcus cells. *International Biodeterioration & Biodegradation*, *63*(4), 427-432.

Kwon, S. M., Kim, H. S., & Jin, H. J. (2008). Fabrication of organic silk fibroin/multiwalled carbon nanotube composite cryogels by freeze-drying method. *Advanced Materials Research*, *47*, 1105-1108.

Lalo, H., Ayela, C., Dague, E., Vieu, C., & Haupt, K. (2010). Nanopatterning molecularly imprinted polymers by soft lithography: a hierarchical approach. *Lab on a Chip*, *10*(10), 1316-1318.

Langer, R. (1993). Polymer-controlled drug delivery systems. *Accounts of chemical research*, *26*(10), 537-542.

Lee, C. (2008). Therapeutic challenges in the era of antibiotic resistance. *International Journal of Antimicrobial Agents*, *32*, S197-S199.

Lode, H. M. (2009). Clinical impact of antibiotic-resistant Gram-positive pathogens. *Clinical microbiology and infection*, *15*(3), 212-217.

Lode, H. M. (2009). Clinical impact of antibiotic-resistant Gram-positive pathogens. *Clinical microbiology and infection*, *15*(3), 212-217.

Loo, S. L., Fane, A. G., Lim, T. T., Krantz, W. B., Liang, Y. N., Liu, X., & Hu, X. (2013). Superabsorbent cryogels decorated with silver nanoparticles as a novel water technology for point-of-use disinfection. *Environmental science & technology*, *47*(16), 9363-9371.

Lopes, G. K., Schulman, H. M., & Hermes-Lima, M. (1999). Polyphenol tannic acid inhibits hydroxyl radical formation from Fenton reaction by complexing ferrous ions. *Biochimica et Biophysica Acta (BBA)-General Subjects*, *1472*(1-2), 142-152.

Lozinsky, V. I. (2002). Cryogels on the basis of natural and synthetic polymers: preparation, properties and application. *Russian Chemical Reviews*, *71*(6), 489-511.

Lozinsky, V. I., & Plieva, F. M. (1998). Poly (vinyl alcohol) cryogels employed as matrices for cell immobilization. 3. Overview of recent research and developments. *Enzyme and microbial technology*, *23*(3-4), 227-242.

Luo, J., Lai, J., Zhang, N., Liu, Y., Liu, R., & Liu, X. (2016). Tannic acid induced self-assembly of three-dimensional graphene with good adsorption and antibacterial properties. *ACS Sustainable Chemistry & Engineering*, *4*(3), 1404-1413.

Ma, L., Feng, S., Fuente-Núñez, C. D. L., Hancock, R. E., & Lu, X. (2018). Development of molecularly imprinted polymers to block quorum sensing and inhibit bacterial biofilm formation. *ACS applied materials & interfaces*, *10*(22), 18450-18457.

Maginnis, M. S. (2018). Virus–receptor interactions: the key to cellular invasion. *Journal of molecular biology*, *430*(17), 2590-2611.

Magri, C., Schridde, U., Murayama, Y., Panzeri, S., & Logothetis, N. K. (2012). The amplitude and timing of the BOLD signal reflects the relationship between local field potential power at different frequencies. *Journal of Neuroscience*, *32*(4), 1395-1407.

McDonnell, G., & Russell, A. D. (1999). Antiseptics and disinfectants: activity, action, and resistance. *Clinical microbiology reviews*, *12*(1), 147-179.

Molinelli, A. (2004). *Molecularly imprinted polymers: Towards a rational understanding of biomimetic materials*. Georgia Institute of Technology.

Mosbach, K., & Ramström, O. (1996). The emerging technique of molecular imprinting and its future impact on biotechnology. *Bio/technology*, *14*(2), 163-170.

Nakamura, Y., Tsuji, S., & Tonogai, Y. (2003). Method for analysis of tannic acid and its metabolites in biological samples: application to tannic acid metabolism in the rat. *Journal of agricultural and food chemistry*, *51*(1), 331-339.

Nishide, H., Deguchi, J., & Tsuchida, E. (1977). Adsorption of metal ions on crosslinked poly (4-vinylpyridine) resins prepared with a metal ion as template. *Journal of Polymer Science: Polymer Chemistry Edition*, *15*(12), 3023-3029.

Okay, O. (Ed.). (2014). *Polymeric Cryogels: Macroporous gels with remarkable properties* (Vol. 263). Springer.

Owens, P. K., Karlsson, L., Lutz, E. S. M., & Andersson, L. I. (1999). Molecular imprinting for bio-and pharmaceutical analysis. *TrAC Trends in Analytical Chemistry*, *18*(3), 146-154.

Palza, H. (2015). Antimicrobial polymers with metal nanoparticles. *International journal of molecular sciences*, *16*(1), 2099-2116.

Palza, H. (2015). Antimicrobial polymers with metal nanoparticles. *International journal of molecular sciences*, *16*(1), 2099-2116.

Park, K. (2014). Controlled drug delivery systems: past forward and future back. *Journal of Controlled Release*, *190*, 3-8.

Peppas, N. A., Bures, P., Leobandung, W. S., & Ichikawa, H. (2000). Hydrogels in pharmaceutical formulations. European journal of pharmaceutics and biopharmaceutics, 50(1), 27-46.

Petrov, P., Utrata-Wesołek, A., Trzebicka, B., Tsvetanov, C. B., Dworak, A., Anioł, J., & Sieroń, A. (2011). Biocompatible cryogels of thermosensitive polyglycidol derivatives with ultra-rapid swelling properties. *European Polymer Journal*, *47*(5), 981-988.

Piletsky, S. A., Alcock, S., & Turner, A. P. (2001). Molecular imprinting: at the edge of the third millennium. *TRENDS in Biotechnology*, *19*(1), 9-12.

Plieva, F. M., Kumar, A., Galaev, I. Y., & Mattiasson, B. (2009). Design of Supermacroporous Biomaterials via Gelation at Subzero Temperatures—Cryogelation. *Advanced Biomaterials: Fundamentals, Processing, and Applications*, 499-531.

Polyakov, M. V. (1931). Adsorption properties and structure of silica gel. *Zhur Fiz Khim*, *2*, 799-805.

Rabieizadeh, M., Kashefimofrad, S. M., & Naeimpoor, F. (2014). Monolithic molecularly imprinted cryogel for lysozyme recognition. *Journal of separation science*, *37*(20), 2983-2990.

Rogers, Z. J., & Bencherif, S. A. (2019). Cryogelation and Cryogels. *Gels (Basel, Switzerland)*, *5*(4), 46.

Sagbas, S., Aktas, N., & Sahiner, N. (2015). Modified biofunctional p (tannic acid) microgels and their antimicrobial activity. *Applied Surface Science*, *354*, 306-313.

Sandle, T. (2014). The Risk of Bacillus cereus to Pharmaceutical Manufacturing. *Am. Pharm. Rev*, *17*(6).

Sellergren, B., & Andersson, L. (1990). Molecular recognition in macroporous polymers prepared by a substrate analog imprinting strategy. *The Journal of organic chemistry*, *55*(10), 3381-3383.

Shea, K. J., & Dougherty, T. K. (1986). Molecular recognition on synthetic amorphous surfaces. The influence of functional group positioning on the effectiveness of molecular recognition. *Journal of the American Chemical Society*, *108*(5), 1091-1093.

Shenai, V.A. (1987). TECHNOLOGY OF TEXTILE PROCESSING VOL-- II chemistry of dyes.

Shirmohammadli, Y., Efhamisisi, D., & Pizzi, A. (2018). Tannins as a sustainable raw material for green chemistry: A review. *Industrial Crops and Products*, *126*, 316-332.

Siddiqui, M. H., Al-Whaibi, M. H., Firoz, M., & Al-Khaishany, M. Y. (2015). Role of nanoparticles in plants. *Nanotechnology and plant sciences: nanoparticles and their impact on plants*, 19-35.

Şener, S., & Yıldırım, M. (2000). Veteriner Toksikoloji. *Teknik Yayıncılık*, *221*, 223.

Takagishi, T., & Klotz, I. M. (1972). Macromolecule-small molecule interactions; introduction of additional binding sites in polyethyleneimine by disulfide cross–linkages. *Biopolymers: Original Research on Biomolecules*, *11*(2), 483-491.

Van Buren, J. P., & Robinson, W. B. (1969). Formation of complexes between protein and tannic acid. *Journal of Agricultural and Food Chemistry*, *17*(4), 772-777.

Wackerlig, J., & Schirhagl, R. (2016). Applications of molecularly imprinted polymer nanoparticles and their advances toward industrial use: a review. *Analytical chemistry*, *88*(1), 250-261.

Wullf, G. (1972). The use of polymers with enzyme-analogous structures for the resolution of racemates. *Angrew. Chem. Int. Ed.*, *11*, 341-341.

Zhang, P., Han, X., Zheng, Y., Wan, J., & Hui, D. (2021). Effect of PVA fiber on mechanical properties of fly ash-based geopolymer concrete. *Reviews on Advanced Materials Science*, *60*(1), 418-437.

Zikmanis, P., Juhņeviča-Radenkova, K., Radenkovs, V., Segliņa, D., Krasnova, I., Kolesovs, S., ... & Semjonovs, P. (2021). Microbial polymers in edible films and coatings of garden berry and grape: Current and prospective use. *Food and Bioprocess Technology*, *14*(8), 1432-1445.